THE UNIVERSITY OF QUEENSLAND

Experimental Investigation of Temperature Effects on Performance of Distributed Acoustic Sensing

Student Name: Nan ZHAO

Course Code: ENGG7290

Supervisor: Associate Professor Saiied Aminossadati

Industry Supervisor: Mr Karsten Hoehn

Submission date: 27 June 2019

Faculty of Engineering, Architecture and Information Technology

EXECUTIVE SUMMARY

Distributed acoustic sensing (DAS) is a novel technology that has been deployed in a board range of industries with a wide variety of applications in geophysical monitoring, pipeline protection, perimeter security and condition monitoring of industrial infrastructures. It has the capability of monitoring acoustic signatures continuously through the entire fibre over vast distances in harsh environments. Many studies have shown that temperature variations result in modifications in physical properties of an optical fibre. To obtain reliable information from the DAS system, it is significant to study if the temperature has an impact on DAS signal transmission. Furthermore, to monitor the condition of applications precisely by using DAS systems, it is necessary to define if the temperature is one of the factors that induce the amplitude variations in the acoustic signatures.

This project aimed to investigate the temperature effects on the performance of DAS. A laboratory experiment and data analysis were conducted to meet the following project objectives:

- to explore the effect of the temperature on frequency characteristics of the DAS system, and
- to examine the impact of the temperature on the amplitude of acoustic signatures.

The results from frequency plots showed that the temperature did not alter the frequency characteristics of the DAS system, but changed the amplitude of the acoustic signatures. The results from the temperature characterisation indicated that the ambient temperature is one of the factors that cause the amplitude variations in the acoustic signatures, but there was no distinctive correlation between them. The potential factors that may have an impact on the outcome of the experiment are identified in the paper. The following recommendations are proposed for future research:

- conducting experiments using different types of optical fibre and comparing the results;
- applying different types of DAS system and comparing the temperature effects on their performance;
- utilising the metal coil with different diameters and comparing the results;
- making sure that the temperature stays constant during the data recording;
- increasing the range of the temperature variation and reducing the temperature interval;
- placing a longer length of the optical fibre in the climatic chamber (minimum: 1.2 km).

ACKNOWLEDGEMENTS

I would like to express my sincere appreciation to my industry supervisor Mr Karsten Hoehn for providing me with the opportunity to do this research project, for his encouragement, continuous support and professional guidance throughout the project.

I would like to express my gratitude to my academic supervisor Associate Professor Saiied Aminossadati, for his valuable comments throughout the project and technical guidance on the thesis.

I would like to extend my gratitude to Dr Christopher Leonardi for his continuous support throughout the placement semester.

I would like to thank Long Giang in Mining3 for providing me with the valuable background of the project, imparting his expertise, and for his technical guidance on signal processing. I would also like to thank Joji Quidim and Dr Paul Wilson in Mining3 for their insightful comments and technical support for the project.

I would like to express special thanks to the University of Queensland, Mining3 and CSIRO for financial support and facility support.

In addition, I would like to express profound appreciation to my mother, Steve and Ryan for their encouragement and support in all possible ways.

CONTENTS

LIST OF FIGURES

LIST OF TABLES

CHAPTER 1 INTRODUCTION

1.1 BACKGROUND

Distributed Acoustic Sensing (DAS) has been rapidly evolving as a compelling and breakthrough fibre-optic based technology with a wide variety of applications. DAS converts an optical fibre into an array of virtual microphones, detecting minute tensions induced by external sound and vibrations along an optical fibre in real time (Kimbell, 2013). DAS system requires an interrogator unit that generates a laser pulse propagating through a single mode optical fibre. The external disturbance enables laser pulses to scatter back along the entire length of the optical fibre towards the interrogator, resulting in light reflections known as Rayleigh backscatter (Jaaskelainen, 2009). The backscatter intensity is measured as a function of time-of-flight based on the principle of coherent optical time domain reflectometry (COTDR). Each backscattered signal is produced under a corresponding "bin" referred to as a discrete range along the fibre with the spatial resolution, which is defined by the laser pulse width (Hill, 2015). DAS technology is capable of monitoring acoustic signatures constantly through the entire fibre over vast distances in harsh environments (Koelman et al., 2011).

In recent years, fibre optic DAS technology with the advantages of non-intrusive, low cost, easy installation and wide monitoring range has become widespread among many applications, such as geophysical monitoring, pipeline protection and perimeter security (Mateeva et al., 2014). In the mining industry, the DAS system has been applied in a conveyor condition monitoring to identify faulty idlers and to detect conveyor belt failure points. A fibre cable which is connected with an interrogator is installed along the conveyor so as to record the acoustic signals from each idler frame (Wilson et al., 2018). To reveal the acoustic signatures of the conveyor rollers and bearings, signal processing is involved to covert the raw data into the frequency domain. Any wear condition of the rollers and bearings is able to be evaluated by analysing the extracted characteristic frequency plots. The severity of the condition is determined by comparing the amplitude of the frequency pattern with a certain threshold (Wilson et al., 2018). However, variations occur occasionally in the amplitude of acoustic signatures that can influence the accuracy of evaluating the wear condition. Many factors potentially cause this issue, but they have not been fully identified yet.

1.2 PROBLEM STATEMENT

Effects of temperature fluctuations on the Rayleigh signal and therefore, the DAS signal was investigated. Research has shown that temperature fluctuations cause changes in the refractive index of an optical fibre, thus changing the speed of light through the fibre (Hartog, 2018). However, DAS systems assume the speed of laser propagating through the optical fibre is consistent. To obtain reliable information from the DAS system, it is significant to study if the temperature has an impact on DAS signal transmission. Furthermore, to monitor the condition of applications precisely by using DAS systems, it is necessary to define if the temperature is one of the factors that induce the amplitude variations in the acoustic signatures.

1.3 AIMS AND OBJECTIVES

The project aims to investigate the temperature effects on the performance of DAS. In order to achieve this aim, the following main objectives are established:

- to explore the effect of the temperature on frequency characteristics of the DAS system by designing and conducting a series of experiments and analysing the processed acoustic data; and
- to examine the impact of the temperature on the amplitude of acoustic signatures via data processing and analysing.

1.4 SCOPE

The inclusions and exclusions of the project are listed and shown in Table 1.1.

Table 1.1. In Scope and Out of Scope of project

In Scope	Out of Scope
Research on the principle of DAS.	Research on the principle of distributed temperature sensing (DTS).
Design and conduct a series of laboratory experiments.	Investigate and test the other effects on DAS.
Collect both raw acoustic sensing data and thermal data from Hawk integration of DAS and DTS interrogator.	Compare the performance of DAS using various types of optical fibre and DAS interrogator.

Process data and generate frequency plots using MATLAB to determine the temperature effects on the frequency characteristic of the system.	Conduct field experiments.
Analyse acoustic signatures to examine the impact of various temperatures on the corresponding amplitude.	Develop signal processing algorithms for DAS and DTS.
Make theoretical calculations of the relationship between the temperature and the refractive index of the optical fibre using experimental parameters.	Develop end-user software.
Compare the theoretical results with the results obtained from experiments.	Calibrate the bin location of the optical fibre in the software.

1.5 SIGNIFICANT TO INDUSTRY

The outcomes of the project would provide the opportunity to allow the processed acoustic signatures more adaptable to the temperature effects, precisely map the discrete range along optical fibre onto the interrogator under temperature variations and make the software a better diagnostic and calibration to optimise the performance of DAS.

1.6 THESIS OUTLINE

The study consists of five chapters, commencing with a background description of DAS systems, a statement of the problem that identifies the purpose of this study and the significance of study outcomes for the industry.

Chapter 2 presents working principles, data acquisition and processing principles of DAS systems, the fundamental principles and the factors that influence the physical properties of the optical fibre. DAS applications, advantages and challenges are also reviewed in this chapter.

Chapter 3 provides details of equipment, setup, conditions and procedures of the laboratory experiment. This chapter also introduces the methodology of data analysis.

Chapter 4 presents and analyses the experiment results corresponding to the project objectives.

Chapter 5 summarises outcomes of the project and provides recommendations for future research.

CHAPTER 2 DISTRIBUTED ACOUSTIC SENSING SYSTEMS

2.1 INTRODUCTION

DAS system is a fibre optic-based acoustic detection technology which has the ability to determine the spatially distributed measurements along a sensing fibre. A single mode optical fibre as the sensing element is connected to a laser source from an interrogator emitting a series of laser pulses (Silkina, 2014). These pulses are launched into the optical fibre and interact with the silica glass in the fibre. The atoms and molecules in the fused silica cause refractive index variations. The acoustic disturbance enables laser pulses to scatter back along the entire length of the optical fibre towards the interrogator, resulting in light reflections known as Rayleigh backscatter (Jaaskelainen, 2009). The Rayleigh backscatter laser signal is precisely mapped to a fibre distance by measuring its arrival time based on the principle of coherent optical time-domain reflectometry (C-OTDR). This chapter aims to provide:

- operational and measurement principles of fibre optic DAS technology,
- performance parameters of DAS,
- DAS data acquisition and signal processing,
- the factors could influence the physical properties of an optical fibre, and
- applications of DAS, their advantages and challenges.

The gaps are identified at the end of the chapter based on the review of the literature.

2.2 PRINCIPLE OF OPERATION AND MEASUREMENT

Fibre optic DAS system is comprised of a fibre optic cable and an interrogator unit, working in conjunction to detect acoustic signals along the cable.

2.2.1 Interrogator Unit

The principal components applied in the DAS interrogator unit is illustrated in Figure 2.1, which consist of a laser source, a pulse generator, an acousto-optic modulator (AOM), a circulator, an avalanche photodiode (APD), an amplifier and a signal processor.

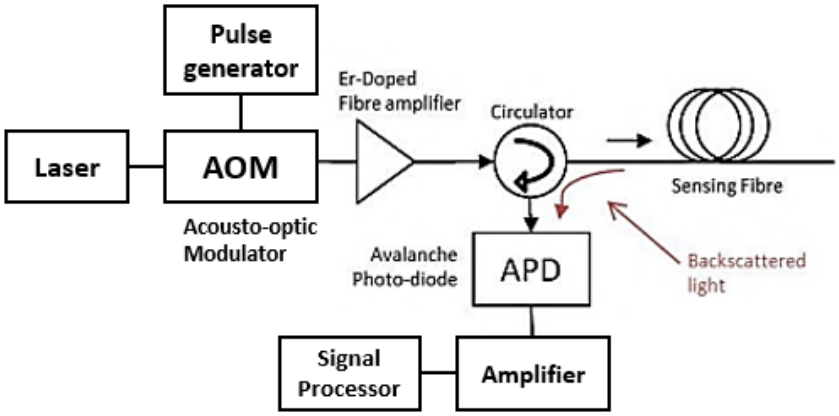

Figure 2.1. Block diagram of C-OTDR based DAS system (Pimentel, 2017).

The C-OTDR based interrogator unit (presented in Figure 2.2) transmits a narrow light pulse generated by the laser source propagating along the fibre and captures the intensity of the Rayleigh-backscattered signals with high sensitivity through a photodetector (Pimentel, 2017). The time it takes from sending the laser pulse to receiving a return Rayleigh backscattered signals is then recorded. As a laser pulse propagates along the fibre, acoustic signals transmitted to the fibre alter scattering properties (Moran). The speed of light through fibre for DAS systems being consistent at approximately two-thirds of the speed of the light through a vacuum can be applied to identify the position of optical loss on the fibre with the return time known as time-of-flight (Systems, 2018). The interrogator employs a combination of Rayleigh backscatter and time of flight to determine the presence, location, intensity and frequency of vibrations along the fibre in real time (Systems, 2018).

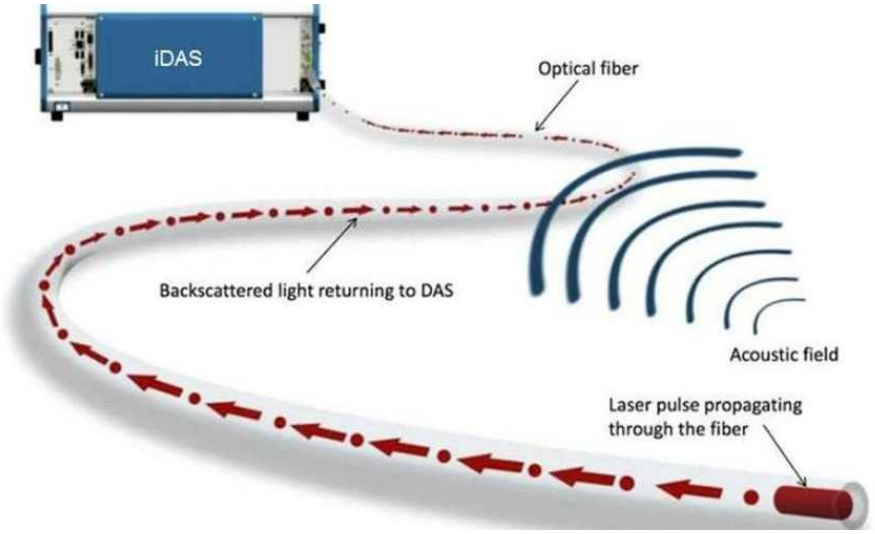

Figure 2.2. Principle of Operation of DAS (Moran).

2.2.2 Data Acquisition and Signal Processing

An interrogator generally has an integrated signal analysis software that rapidly records, processes and analyses the raw data from the system, as well as detects and reports acoustic inputs and vibrations (Hawk, 2017). The data is displayed in a waterfall graph with the x-axis being fibre distance, y-axis being time and the colour representing the recorded signal intensity (Cannon and Aminzadeh, 2013). The operator is able to monitor any discrete range along the fibre. The waterfall display is adequate for most applications of DAS. However, to make the raw data meaningful for varies applications, it is necessary to extract and process the raw data using specific data processing algorithms and techniques such as Fast Fourier Transform and filtering.

Pulse width, spatial resolution and sample rate are some of the essential performance parameters for DAS systems. Pulse width known as laser pulse duration must be long enough to guarantee that the laser produces adequate energy in order for the reflection to be detected by the receiver (Systems, 2018). The longer the pulse width, the more backscatter to be detected; however, the longer the pulse width, the longer section of fibre that responds to acoustic inputs and vibrations (Systems, 2018). The range resolution of the system mainly depends on the pulse width and the speed of light in the fibre, which can be obtained by using Equation 1:

$$\Delta R = \frac{\tau \times v}{2} \qquad \text{Eq. (1)}$$

where ΔR is the range resolution, τ represents the transmitted pulse width, and v is the speed of light in the fibre.

The sample rate defines the number of pulses emitted from the laser per second and determines the delay between two pulses (Systems, 2018). The selection of the sample rate is required to base on frequencies produced under application conditions. The maximum frequency that the system can detect is half the sample rate following the rule of the Nyquist theorem. The amount of time it takes for the laser pulse to propagate along the fibre is determined by the speed of light in fibre and the length of the fibre. Thus, to attain the same dynamic range, the sample rate is inversely proportional to the length of the fibre.

2.2.3 Optical Fibre

An optical fibre is made of pure silica glass (silicon dioxide). The general structure of an optical fibre cable includes a core, cladding, coating and jacket shown in Figure 2.3. The amount of light

absorption depends on the purity of the glass fibre. The relationship between the refractive index and the speed of light travelling through the glass fibre is expressed as:

$$n = \frac{c}{v} \qquad \text{Eq. (2)}$$

where n represents the refractive index of the glass fibre, c is the speed of light in vacuum and v is the speed of light in the glass fibre. The fibre jacket is made up of plastic, protecting the optical fibre from environmental and physical damage.

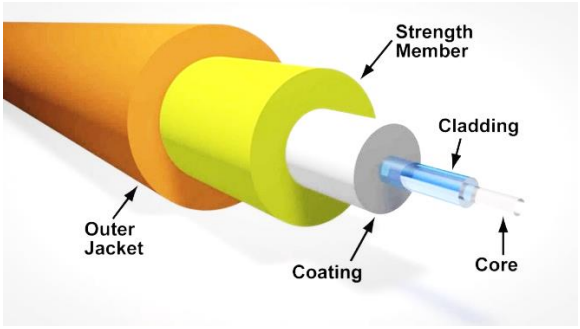

Figure 2.3. The structure of an optical fibre (Hussaini, 2017).

Optical fibre falls into three categories: single mode fibre, multimode step index fibre and multimode graded index fibre. The structure of these types of fibre is illustrated in Figure 2.4. Single mode fibre is currently employed for DAS systems, whereas the multimode optical fibre is mostly applied in DTS systems.

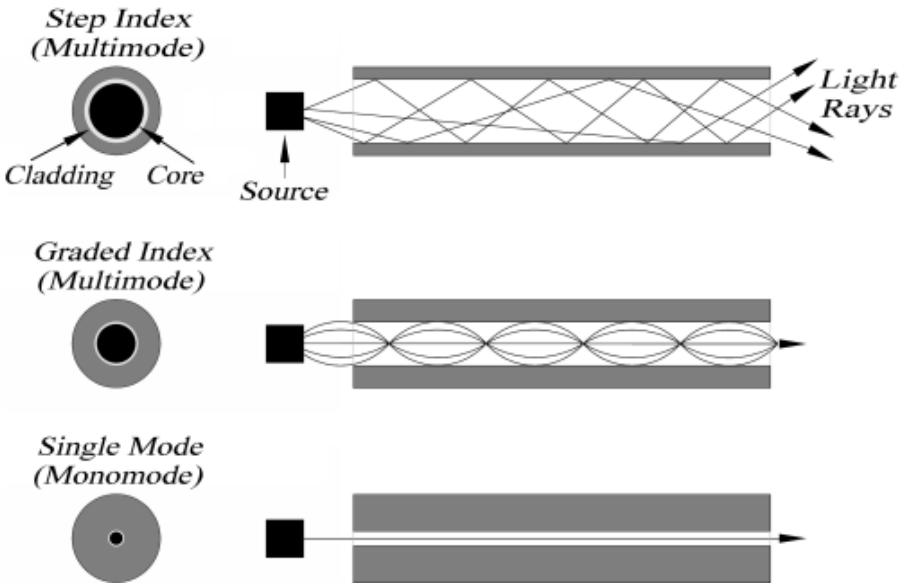

Figure 2.4. The structure of multimode step index optical fibre, multimode graded index optical fibre and single mode optical fibre (Liu, 2014).

The core glass of a single mode fibre is approximately 3 to 10 μm in diameter, which is around ten times narrower than that of a multimode fibre (Liu, 2014). Only a single path is allowed for the light in the single mode fibre to transmit, eliminating the light pulse dispersion. These features make the single mode fibre possess a larger bandwidth and higher propagation speed (Liu, 2014). The performance of optical fibres can be improved by increasing the pulse transmission rate, which is achieved by shortening the pulse duration within limits (Ismail, 2009).

2.3 FIBRE CHARACTERISATION

The main part of the DAS system is an optical fibre. In order to achieve the best performance of DAS in various applications, it is significant to identify the factors that have an impact on fibre characterisation. This section focuses on reviewing the effects of the wavelength of the light and temperature on the refractive index of fibre and the thermal effects on properties of optical fibre.

2.3.1 Characterisation of Optical Refractive Index

From Equation 2, it is known that the refractive index is inversely proportional to the velocity of light in the glass fibre. The relationship between the wavelength of the light (λ) and the velocity of light through the fibre (v) is given by:

$$v = f\lambda \qquad \text{Eq. (3)}$$

where f is the frequency.

Then the equation for the refractive index and the wavelength becomes:

$$n = \frac{c}{f\lambda} \qquad \text{Eq. (4)}$$

Equation 3 demonstrates that for the silica glass optical fibre, the refractive index is inversely proportional to the wavelength of light.

By verifying the theory, Jasny et al. (2004) conducted an experiment by measuring the refractive index of fused silica with the UV light from 346 to 380 nm at temperatures from 143 K to 293 K. The experiment result shown in Figure 2.5 supported the theory that the refractive index of fused silica decreases with increasing of the wavelength.

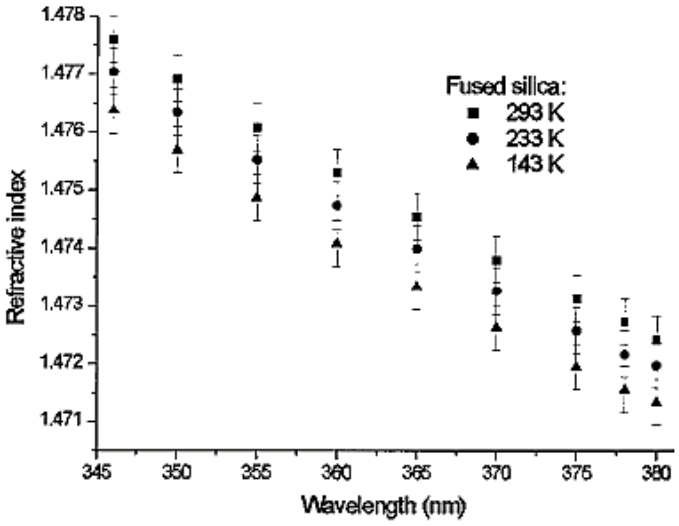

Figure 2.5. A plot of the refractive index of fused silica as a function of wavelength at 143 K, 233 K and 293 K (Jasny et al., 2004).

It can also be seen in Figure 2.5 that the refractive index changes with changing of the temperature. Jasny et al. (2004) generated a plot for the refractive index of fused silica as a function of temperature, as shown in Figure 2.6. It is shown that the refractive index of fused silica has a linear relationship with the temperature. A mathematical expression was obtained from the study of Jasny et al. (2004), as shown in Equation 5:

$$n_{silica}(T) = (7.83 \pm 0.99) \times 10^{-6}\, T + 1.47219 \pm 2.2 \times 10^{-4} \qquad \text{Eq. (5)}$$

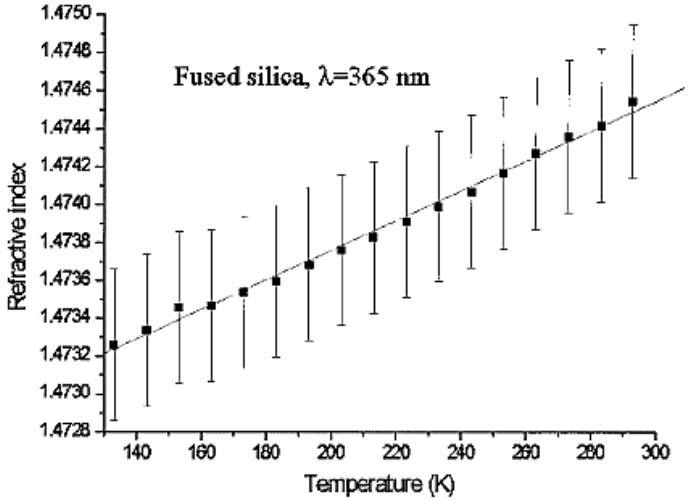

Figure 2.6. A plot of the refractive index of fused silica as a function of temperature as the wavelength of the light being 365 nm (Jasny et al., 2004).

A theoretical model for presenting the relationship between the refractive index of fused silica (n) and the ambient temperature (T) in Kelvin was developed by Wang et al. (2014), as shown in Equation 6:

$$n \approx 7.0978 \times 10^{-6}\mathrm{T} + 1.47269 \qquad \text{Eq. (6)}$$

The theoretical model was compared with the experimental result obtained by Jasny et al. (2004), further demonstrating that the refractive index of the glass fibre is linearly proportional to the temperature (Wang et al., 2014).

2.3.2 Thermal Effects on Properties of Optical Fibres

A study of Yeung and Johnston (1978) aimed to investigate the temperature effects on the transmission properties of various optical fibres. The experiments were carried out by testing different types of single-mode fibre in a temperature controlled chamber with the temperature range between -150°C and 30°C and in an oven with the temperature from 25°C to 150°C severally (Yeung and Johnston, 1978). The results indicated that the transmission power of silicone-cladding fibres was deficient as the temperature was below around -50°C due to the changing of the refractive index in the cladding, which implied that the silicone-clad fibre was not applicable to light transmission in this environment (Yeung and Johnston, 1978). Yeung and Johnston (1978) also tested temperature effects on the refractive index of various optical fibre. The result presented that the refractive index of the polymer-cladding fibre increased with decreasing temperature. The experiment results confirmed that the transmission loss was not affected by the fibre length, but caused by the numerical aperture of the fibre reduced with the decreasing refractive index (Yeung and Johnston, 1978).

By knowing that the refractive index of the fibre can be expressed as a function of temperature (Equation 6), the time-of-flight (t) a laser pulse propagates through a fibre along a certain distance (d) is given by:

$$\mathrm{t} = \frac{d}{v(T)} = \frac{d \times n(T)}{c} \qquad \text{Eq. (7)}$$

Thus, the change in the time-of-flight (Δt) due to the change in refractive index becomes:

$$\Delta\mathrm{t} = \frac{d \times \Delta n(T)}{c} = \frac{d}{\Delta v(T)} \qquad \text{Eq. (8)}$$

Tateda et al. (1980) studied the thermal characteristic of the phase shift in bare and jacked optical fibres both theoretically and experimentally. The phase shift caused by the change of temperature can be interpreted as the delay time of an optical pulse, as shown in Equation 8 (Tateda et al., 1980). The results obtained from both the frequency method and pulse method indicated that the thermal effect on jacketed fibres is much higher than that on bare fibres (Tateda et al., 1980).

Katsuyama et al. (1980) investigated the optical loss characteristics of coated single-mode fibres. It was found that transmission loss for the coated single mode fibre increased steeply at low temperatures (Katsuyama et al., 1980).

Golnabi and Sharifian (2013) reported that the optical loss is affected by the fibre dimension, materials, the radius of the bent fibre and the wavelength of the light. The experimental setup is shown in Figure 2.7, where the light source used in the experiment was a white LED, and laser diode and the temperature was in a range from 20°C to 60°C (Golnabi and Sharifian, 2013).

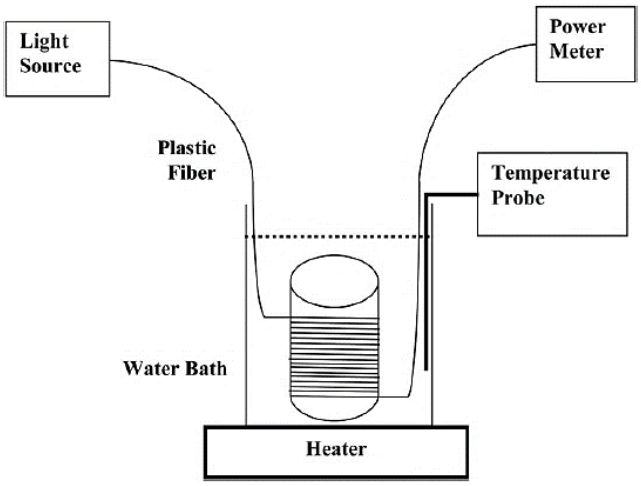

Figure 2.7. Setup of the experiment carried out by Golnabi and Sharifian (2013).

The result in Figure 2.8 shows that the transmitted power of a rolled fibre is lower than that of an unrolled fibre, indicating that the bent fibre can result in fibre transmission loss. The other outcome of the experiment demonstrated that the transmitted power for a bent fibre varied with the temperature of the fibre (Golnabi and Sharifian, 2013).

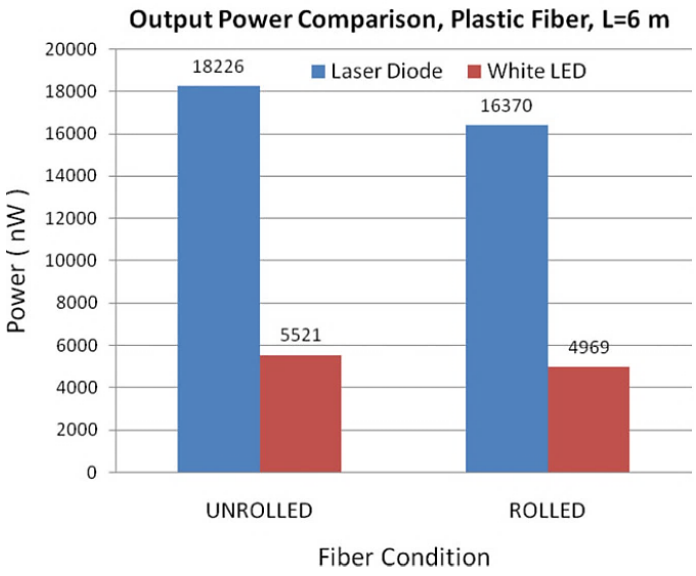

Figure 2.8. The transmitted power comparison of the unrolled fibre and the rolled fibre using laser diode and white LED (Golnabi and Sharifian, 2013).

2.4 APPLICATIONS

DAS is a rapidly evolving fibre-optic technology with numerous advantages widely applied in geophysical monitoring, pipeline protection, perimeter security and condition monitoring in mining industries.

2.4.1 Geophysical Monitoring

Mestayer et al. (2011) investigated the feasibility of utilising DAS as a Measurement-Monitoring-Verification tool to record vertical seismic profile (VSP) data in a well and compared it with the conventional geophones. Results obtained from the field experiment indicated that DAS with the advantages of low cost, simplicity and non-intrusiveness was a feasible alternative for acquiring VSP data in down-hole geophysical surveillance (Mestayer et al., 2011). However, the frequency spectra result for the deep portion of the well in Figure 2.9 showed that the signal to noise ratio of DAS was lower than that of the geophone (Mestayer et al., 2011). The weakness of DAS was predicted to be caused by the weak sensitivity to reflections in the deep portion of the well.

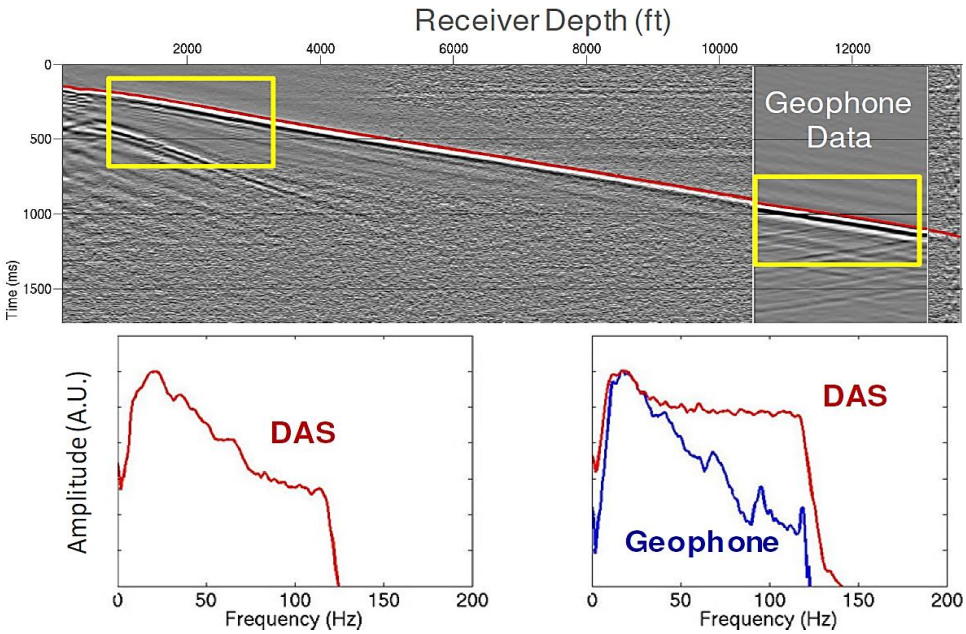

Figure 2.9. The comparison of the frequency spectrum and the noise floor for DAS and geophone at shallow (left) and the deep (right) portion of the well (Mestayer et al., 2011).

A study conducted by Molenaar et al. (2012) aimed to reinforce the detection and comprehension of hydraulic fracture treatments, using a combination of DTS and DAS. By observing the location and intensity of the noise from the waterfall graph of fluid flow, the events for the dropping of balls and the number of fluids for each hydraulic fracture stage could be identified and quantified. The results obtained from the two case studies demonstrated that the DTS and DAS measurements were beneficial to improving real-time hydraulic monitoring and the execution of fracture stimulation (Molenaar et al., 2012).

Daley et al. (2013) conducted a series of field tests applying DAS technology to acquire seismic data in both borehole and surface. In the first field test, the fibre cable was deployed in a 2.9 km well with a short string of clamped geophones (Daley et al., 2013). The results indicated that the DAS system effectively monitored the seismic energy; however, compared to geophones, the DAS recorded data showed that the fluid-coupled fibres were relatively low in sensitivity and the signal to noise ratio was not sufficient to survey P-waves deeper than approximately 1600 m (Daley et al., 2013). In the last two field tests, both DAS sensitivity and signal to noise ratio were improved by replacing the previous fibre deployment with multiple runs of fibre and a loop of fibre cable cemented in place (Daley et al., 2013).

In order to further enhance the signal to noise ratio of DAS, Li et al. (2015) suggested in the paper that a stronger acoustic source can be employed to minimise the noise floor of the interrogator unit,

and some signal processing techniques such as band-pass filter, median filter, wavelet and curvelet transform can be applied to remove the random noise and extract the expected signals in DAS measurements (Li et al., 2015).

2.4.2 Pipeline Protection

The third-party intrusion and fluid leaks, presenting a significant safety and environmental threat, are the most frequent cause of failure in oil and gas pipelines. However, the conventional approaches for protecting pipelines have been demonstrated to be deficient in leak detection and damage prevention. Giunta et al. (2011) and Tejedor et al. (2016) performed a field test severally by deploying the optical fibre along a certain distance of the pipeline section with DAS technique to identify the simulated third-party intrusion and leak events. The spectrogram of the pressure signal, histogram and waterfall graphs for several channels were analysed in the study of Giunta et al. (2011), showing that fibre optic DAS was able to detect, locate and classify the early stage of threats to the pipeline (Giunta et al., 2011). By evaluating and comparing various techniques of position selection and normalization, 8 out of 10 threat events were accurately recognised and 4 out of 10 times that the system presented a false positive (Tejedor et al., 2016).

In order to demonstrate the feasibility of DAS monitoring system for pipelines in the oil and gas industry, conditions of the pipeline were monitored in the project of Hussels et al. (2016) by detecting acoustic signals in the environment of pipes using DAS system. Two sections of the optical fibre as sensors were installed in a 1 m steel pipe, as shown in Figure 2.10. The two sensor sections were separated by 30 m of fibre to prevent the backscattered signals generated in different sections from overlapping (Hussels et al., 2016). The signal generator was applied to produce sinusoidal test signals in a range of kHz to a piezo speaker that was pressed against the surface of the pipe (Hussels et al., 2016). C-OTDR based DAS system was set with a sample rate of 42 kHz and the pulse width ranging from 30 ns to 100 ns.

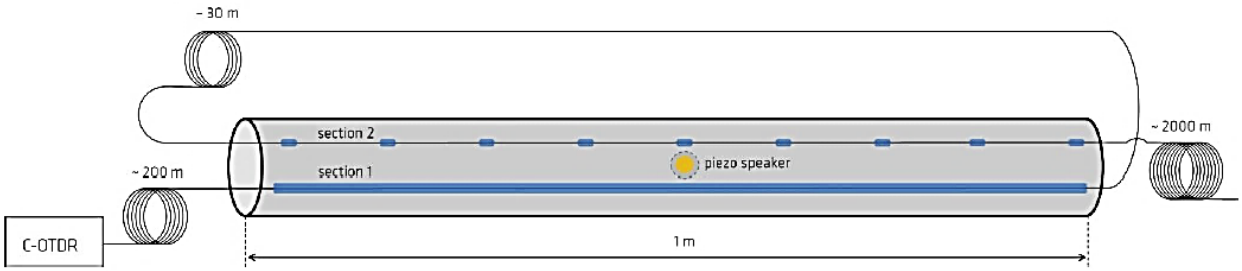

Figure 2.10.Schematic of the experimental setup for condition monitoring of the pipeline (Hussels et al., 2016).

The acoustic signatures shown in Figure 2.11 were obtained by processing the raw acoustic data via fast Fourier transform (FFT) in time intervals of 0.05 s, illustrating that the signal intensity for section 1 was approximately 20 times higher than that of section 2 (Hussels et al., 2016). The comparison plot shown in Figure 2.11 indicated that the peak signal intensity for 100 ns is higher by a factor of approximately 3.8 than that for 30 ns (Hussels et al., 2016).

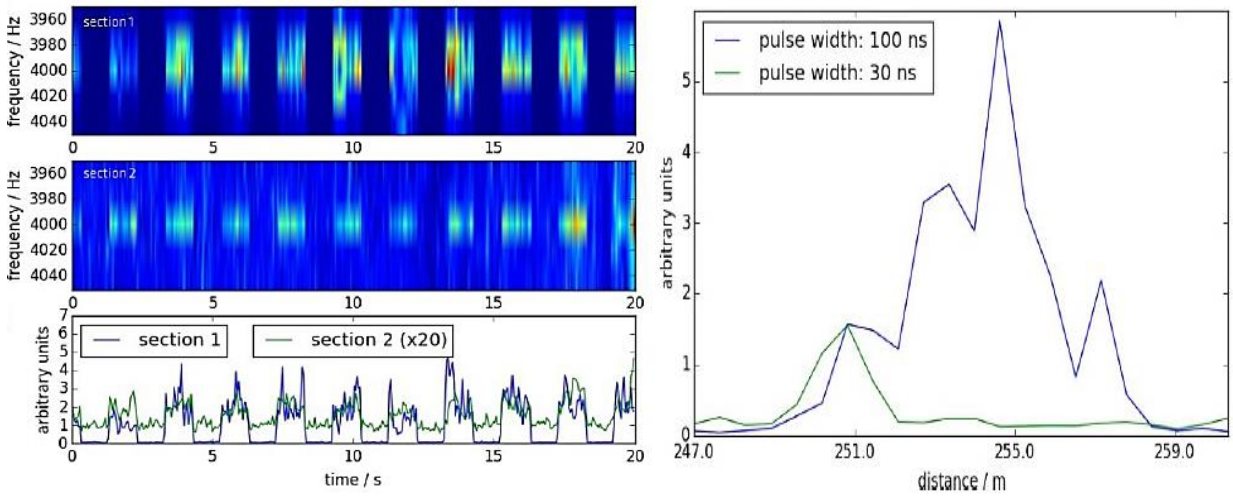

Figure 2.11. Acoustic signatures (frequency vs. time) for the two sensor sections and a plot for comparing the signal intensity at 4 kHz of the two sensor sections are presented on the left-hand side. A plot on the right-hand side is for comparing the signal intensity at 4 kHz as the pulse width being 100 ns with that as the pulse width being 30 ns (Hussels et al., 2016).

These results revealed that the entire length of the optical fibre needs to be attached to the surface of the pipe (as the setup of section 1 in Figure 2.10) to ensure optimal acoustic signal transmission, and the short optical pulses can be used to achieve a high spatial resolution (Hussels et al., 2016). However, in order to make the fibre optic DAS system fully adapt to pipeline applications, the temperature effects on adhesives and the coating material are necessary to investigate, and different DAS configurations for the pipeline monitoring need to be explored (Hussels et al., 2016).

2.4.3 Security Monitoring

The installations for both commercial and governmental perimeter security are generally comprised of multiple sensors. Duckworth and Ku (2013) introduced an installation of DAS combining with fence sensors and multiple video cameras, which was able to provide early warning of threat activities at a perimeter boundary. DAS technology applied in perimeter monitoring not only enhances security but also reduces operating expenses (Duckworth and Ku, 2013).

He et al. (2018) investigated the reliability of DAS applying to the railway intrusion detection by conducting a one-week field test. The DAS was performed with a spatial resolution of 10 m and the total sensing distance of 9 km (He et al., 2018). Video cameras were used to verify the DAS alarms. The results showed that all the intrusion events were detected and low false alarm frequency was occurred during the field test, demonstrating the high reliability of using DAS system for monitoring the intrusion into the railway (He et al., 2018).

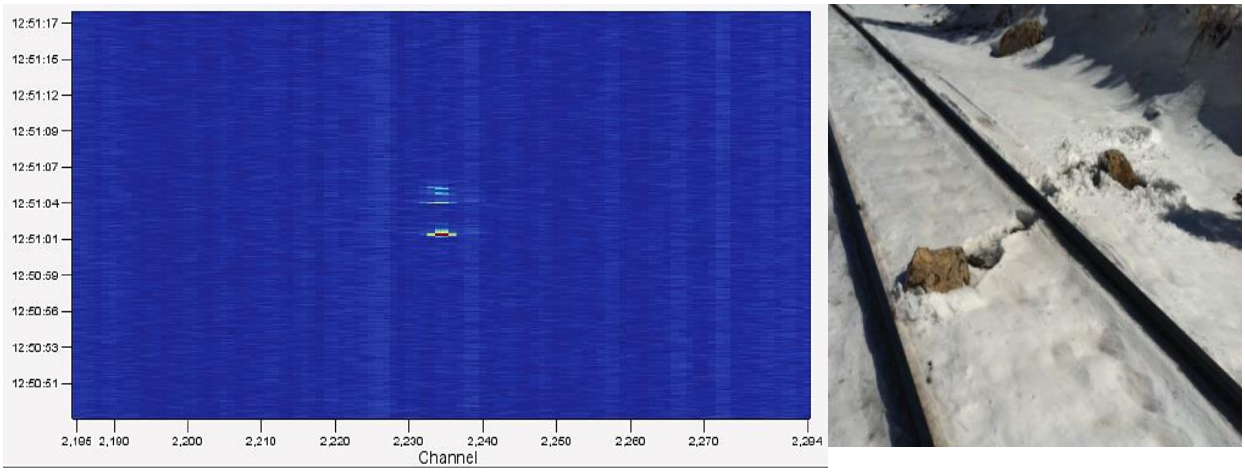

Figure 2.12. The rock fall event (right) and the corresponding waterfall graph (left) (Akkerman and Prahl, 2013).

In addition to the perimeter security, the DAS system can also be implemented to the railroad for detecting, locating and alarming on rock falls. A waterfall graph (shown in Figure 2.12) generated from DAS system with the vertical axis being time and the horizontal axis being the channel number displays the track of falling rocks and the location of the rockfall event (Akkerman and Prahl, 2013). By conducting a series of field tests, the average nuisance alarm rate (NAR) obtained by Akkerman and Prahl (2013) was approximately one per day. However, the NAR became higher during the changing seasons, which was caused by temperature fluctuations increasing the thermal expansion and contraction of the railway track. (Akkerman and Prahl, 2013).

2.4.4 Condition Monitoring in Mining Industry

A typical conveyor in underground coal mine can have up to 6,000 bearings per kilometre, making the bearing failure detection in conveyor rollers especially tricky, time-consuming and labour intensive (Wilson et al., 2016). A DAS-based conveyor monitoring system (Figure 2.13) as a newly emerging solution was developed for assisting the conveyor maintenance. It is demonstrated that the DAS technology is capable of monitoring the health of the rollers in every section of the conveyor, detecting the different stages of wearing rollers and determining the type of idler damage (Wilson et al., 2016).

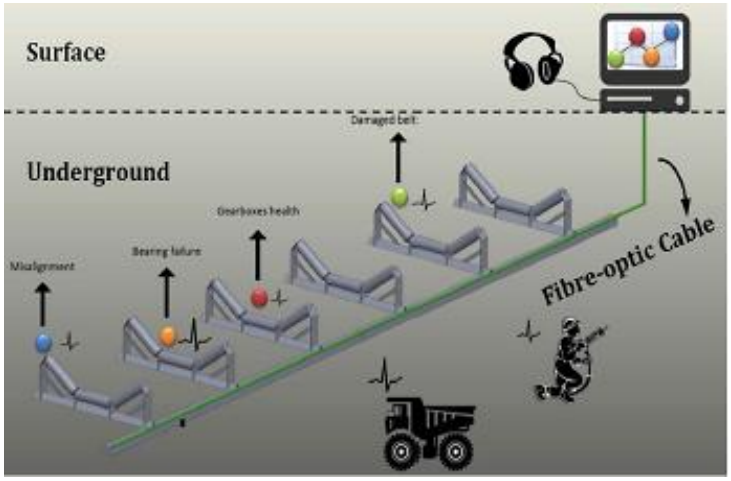

Figure 2.13. The layout of the DAS-based conveyor condition monitoring system (Wilson et al., 2016).

Hicke et al. (2017) investigated the usability of DAS for acoustic condition monitoring of rollers in conveyor belt systems in the mining industry by diagnosing three different representative rollers in an acoustic test stand (Hicke et al., 2017). Figure 2.14 shows the setup of one of the rollers in the acoustic test stand that was acoustically isolated from the external environment. A DAS system was applied using the optimal pulse width for measuring the acoustic signals. The time-dependent spectrograms in Figure 2.14 illustrate that the worse the roller damaged, the broader the acoustic emission spectrum. The result demonstrated that the DAS is applicable to machine condition monitoring, and the spectrogram can be used as an indicator of the condition of industrial infrastructures (Hicke et al., 2017).

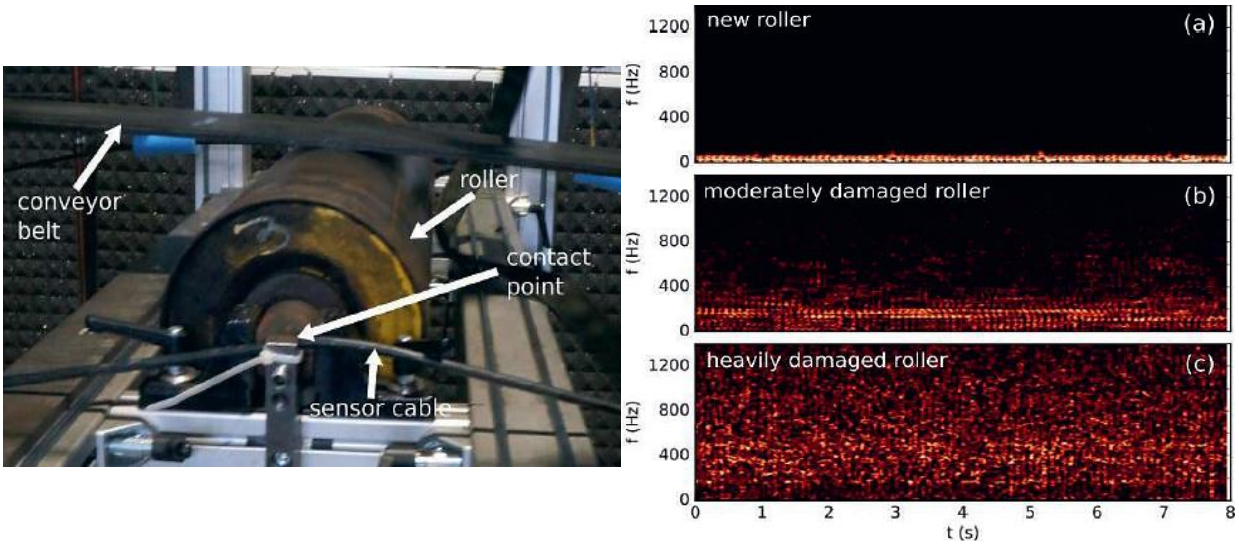

Figure 2.14. Setup for one of the examined conveyor rollers in the acoustic test stand (left) and the time-dependent acoustic signatures (right) for (a) new roller (b) moderately damaged roller and (c) heavily damaged roller (Hicke et al., 2017).

However, in the real-life condition, the conveyor cannot be fully isolated. Hicke et al. (2017) found that applying the DAS condition monitoring system in the temperature unstable environments would result in low DAS sensitivity and even total loss of sensitivity.

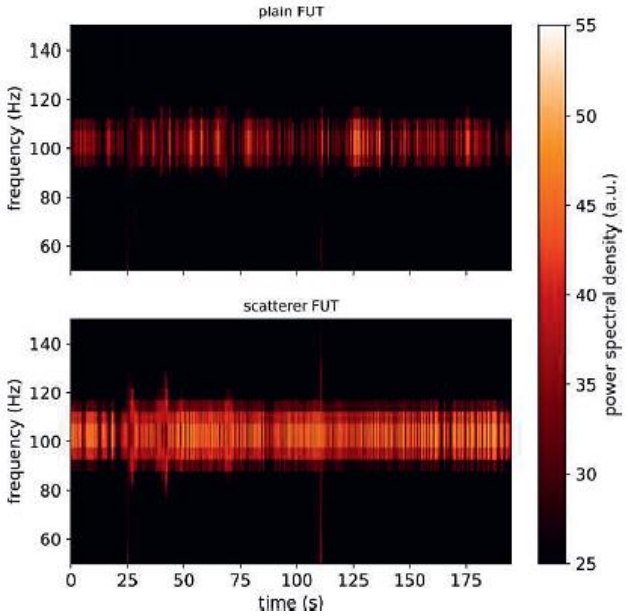

Figure 2.15. Spectrograms for the original optical fibre and the modified optical fibre, with an input acoustic frequency of 100 Hz (Hicke et al., 2017).

A possible solution for it was to modify the fibre segment and increase the amplitude of backscattering (Hicke et al., 2017). For validating this method, an experiment was conducted by measuring the acoustic signal from an original fibre and a modified fibre under a 2°C fluctuating temperature environment. A function generator was used to produce an input frequency of 100 Hz with a voltage amplitude of 200 mV. The outcome displayed in Figure 2.15 shows that the fibre with altered backscattering has a higher power spectral density (PSD) in average, which implies that DAS sensitivity was enhanced (Hicke et al., 2017).

2.5 RESEARCH GAP

In the review of previous research on temperature effects on properties of an optical fibre and applications of the DAS system, several research gaps are identified as follows:

- an investigation of thermal effects on the frequency characteristic of the DAS system; and
- a study on thermal effects on the amplitude of DAS acoustic signatures.

CHAPTER 3 EXPERIMENTAL METHODOLOGY

3.1 INTRODUCTION

This chapter provides detailed experimental setup, including the introduction to the apparatus applied in the laboratory experiment, equipment selection and layout. The experiment conditions, an overview of experimental procedure and data analysing methodology are also described in the chapter.

The equipment used in the laboratory experiment includes:

- an ACS climatic test chamber
- a 4-inch woofer speaker,
- a TTI 40 MHz DDS function/arbitrary generator,
- two 20 m long single-mode optical glass fibre,
- two aluminium coils with a diameter of 9.6 cm,
- a Polyurethane foam soundproofing sheet, and
- a Hawk Praetorian Fibre Optic Sensing DAS/DTS Sensing system.

3.2 EXPERIMENTAL SET-UP

3.2.1 Climatic Test Chamber

An ACS climatic test chamber shown in Figure 3.1 is safety and eco-friendly innovation, allowing both temperature and humidity to be controlled within limits:

- the temperature range is between -40°C and 200°C, fluctuating between ±0.1°C and ±0.3°C; and
- the relative humidity is in the range of 10% to 98%, fluctuating between ±1% and ±3%.

A cable notch located on the side of the door provided a space for connections to the exterior of the chamber. A test tray inside the chamber allows the objects on it to receive uniform temperature and humidity gradient.

Figure 3.1. ACS climatic test chamber.

3.2.2 Distributed Acoustic Sensing System

HAWK Praetorian Fibre Optic Sensing DAS/DTS system shown in Figure 3.2 allows applications such as pipelines, railways and conveyors to be measured in real time by detecting distributed disturbances that occur in a fibre optic cable attached to the application (Hawk, 2017).

The system converts a single-mode fibre optic core into numbers of microphones and thermometers (presented in Figure 3.2), detecting, locating and analysing sounds, vibrations and different temperature at every half meter (the size of the bin) along the fibre (Systems, 2018). The speed of light through a fibre is assumed to be consistent in the DAS system at approximately two-thirds of the speed of light through a vacuum (Systems, 2018). The DTS system scans through various temperatures along with the optical path, providing temperature profiles of the fibre at every point along the application (Systems, 2018).

The fundamental system specifications are:

- the maximum detectable optical path range of DAS is 40 km, and
- the maximum sample rate when the length of fibre < 833 m is 120,000 Hz (Systems, 2018).

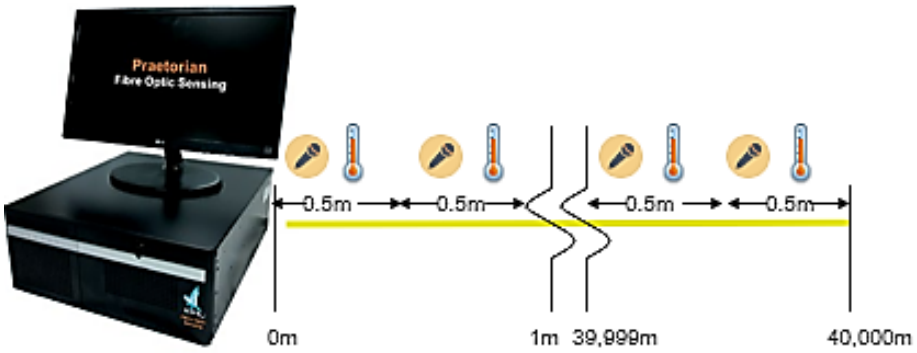

Figure 3.2. HAWK Praetorian Distributed Acoustic and Temperature Fibre Optic Sensing system and its functional diagram (Systems, 2018).

3.2.3 Speaker and Function Generator

A 4-inch woofer speaker connecting with a 40 MHz DDS function/arbitrary generator (shown in Figure 3.3) produces acoustic signals with different frequencies.

Figure 3.3. A 4-inch woofer speaker is attaching to a TTI 40 MHz DDS function/arbitrary generator.

The key specifications of the speaker and function generator are summarised in Table 3.1 and Table 3.2, respectively.

Table 3.1. 4-inch woofer speaker specifications.

Parameter	Value	Unit
Frequency Response	70 – 7000	Hz
Resonant Frequency	59.9	Hz
Nominal Impedance	8	Ω
RMS Power Rating	27	W

Table 3.2. 40 MHz DDS function/arbitrary generator specifications.

Parameter	Value	Unit
Frequency Range	1 – 40	mHz – MHz
Resolution	1	mHz
Harmonic Distortion to 20 kHz	<-60	dBc

3.2.4 Apparatus Set-up

Figure 3.4 illustrates the overview of apparatus setups and explicit connections between each equipment. The interior installation of the climatic chamber is displayed in Figure 3.5a. Two 20 m single-mode fibre cables, beginning with 5 m from the cable aft, were looped on the aluminium coils separately. 1.7 m of the fibre cables were formed into a DAS fibre coil and a DTS fibre coil, locating on the test tray of the chamber. 8 m of the DAS fibre in total were placed in the chamber, as shown in Figure 3.6.

Polyurethane foam was placed at the bottom of the DAS fibre coil to minimise vibrations from the chamber. The speaker with its membrane downwards was installed on the top of the DAS fibre coil, ensuring that the consistent frequency and signal intensity were received at every point along with the fibre coils. A BNC to alligator clip cable was used to connect the speaker to the function generator through the cable notch, as shown in Figure 3.5b.

Two fibre coils were connected through the cable notch to the Hawk DAS/DTS interrogator unit, as shown in Figure 3.4 and Figure 3.5c so that acoustic and thermal signatures could be monitored and recorded. The thermal signatures were used to compare the temperature in the chamber with the actual temperature that the fibre received.

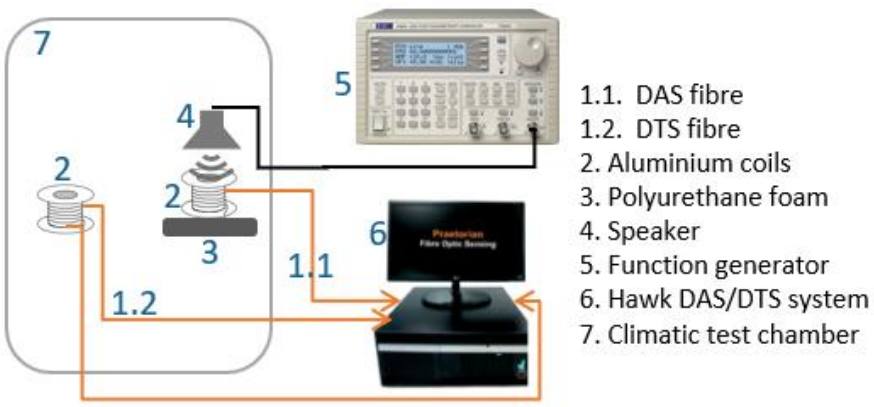

Figure 3.4. The layout of the laboratory experiment.

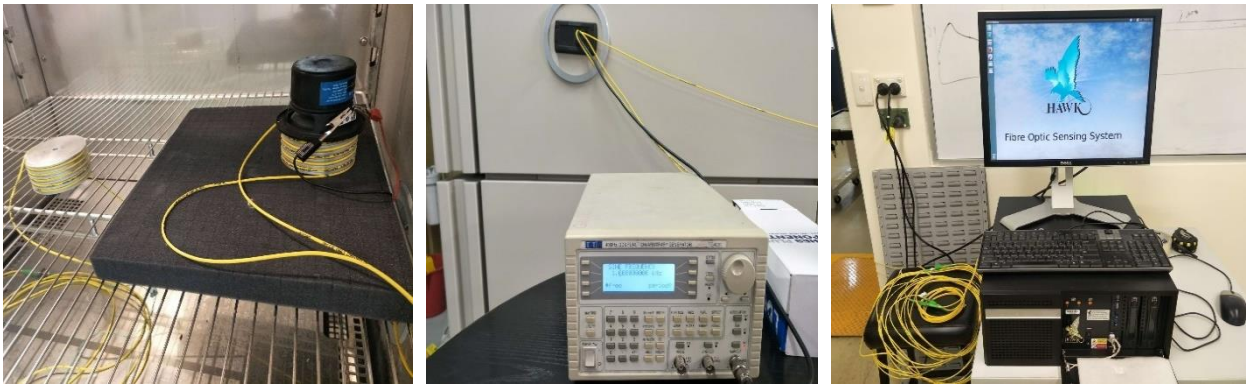

(a) (b) (c)

Figure 3.5. (a) Installations inside the climatic chamber (b) Function generator installation (c) Hawk DAS/DTS system was installed in a control room next to the climatic chamber.

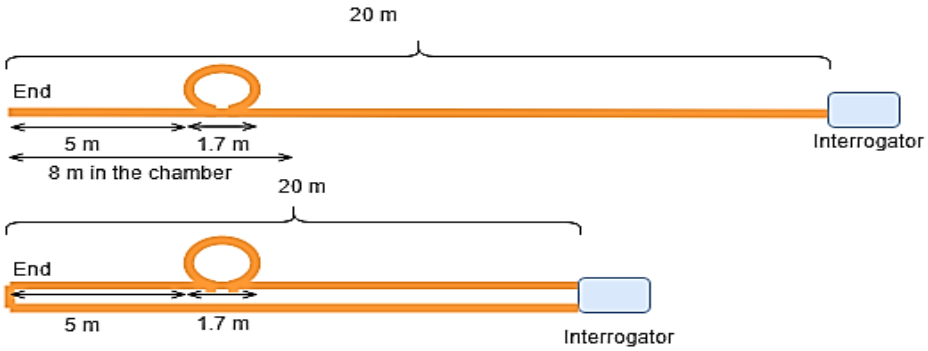

Figure 3.6.Outline of DAS (top) and DTS (bottom) fibre installations.

3.3 EXPERIMENTAL CONDITIONS

Table 3.3 presents the configuration of independent variables that were the input frequency of the function generator and ambient temperatures inside the climate chamber in the experiment. The function generator produced an input sine wave ranging from 100 Hz to 1500 Hz that were in the range of the speaker frequency response shown in Table 3.1. The temperature of the climatic test chamber was set within limits.

Table 3.3. Independent variable settings.

Parameter	Range	Interval	Unit
Input Acoustic Frequency (sine wave)	100 – 1500	100	Hz
Temperature	-10 – 50	10	°C

Experiment control variables and their settings are summarised in Table 3.4. The relative humidity in the climatic chamber was controlled at 50% with an accuracy of ±2% as the temperature above 0°C, however, when the temperature in the chamber below 0°C, the humidity could not be controlled. The input voltage from the function generator was tested to be at least 4 V to produce detectable acoustic intensities. The laser pulse width was selected based on spatial resolution. According to Equation 1, 5 ns pulse width provided 0.5 m range resolution that was the same as the system spatial resolution. The selection of the sample rate was chosen based on the input acoustic frequency transmitted to the fibre. Table 3.3 shows that the maximum acoustic frequency in the experiment was 1500 Hz; thus, the sample rate had to be equal or higher than twice of the maximum acoustic frequency following the rule of the Nyquist theorem. 5 min recording time with the climatic chamber turned off was sufficient to record raw acoustic data; however, the temperature of the chamber could decrease by 1°C to 2°C within the period.

Table 3.4. Experimental control variable settings.

Apparatus	Parameter	Value	Unit
Climatic Test Chamber	Relative humidity (For temperatures above 0°C)	50 ± 2	%
Function Generator	Input acoustic voltage	4	V
Interrogator	Spatial resolution (size of the bin)	0.5	m
	Laser pulse width	5	ns
	Sample rate	5	kHz
	Temperature resolution	1	°C
	Data recording time	5	min

3.4 EXPERIMENTAL PROCEDURES

Figure 3.7 presents the overall experimental procedures for the project. At first, a ‘tap test’ was done by taping the coiled fibre cable and recording their corresponding bins to match the actual location of the DAS fibre coil with the positions along the fibre in the system. All the control variables were set after the tap test. Then, the temperature of the chamber was set at -10°C and the function generator was initially turned off. Once the temperature became stable, the chamber was paused, and DAS/DTS data were recorded for 5 minutes as the reference data. Next, the input

frequency was regulated from 100 Hz to 1500 Hz, incrementing 100 Hz each time, and DAS/DTS data were recorded 2 times with the climatic chamber turned off. The chamber was restarted to reach the required temperature if the temperature of the climatic chamber tended to decrease

The third stage shown in Figure 3.7 was repeated for the chamber temperature varying from -10°C to 50°C with 10°C interval.

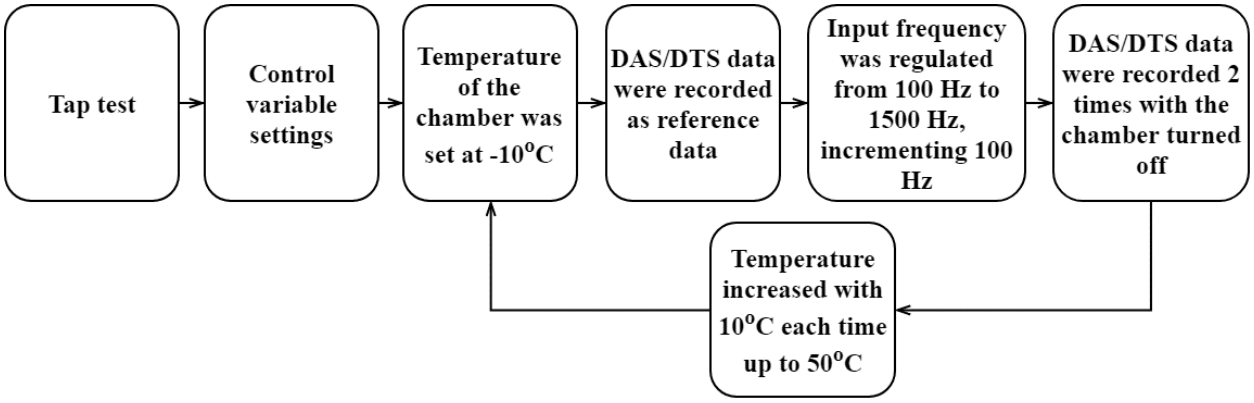

Figure 3.7. A flow chart for experimental procedures.

3.5 DATA ANALYSING METHODOLOGY

The outline of the data analysing methodology applied in the project is shown in Figure 3.8. In order to produce frequency plots for each bin, the saved acoustic raw data that was in the time domain was pre-processed and post-processed using the processing algorithms supplied by Mining3. The frequency resolution was calculated to be:

$$Frequency\ Resolution = \frac{\frac{Sample\ Rate}{2}}{\frac{Number\ of\ Samples}{2}} \approx 0.0763 \text{ Hz}$$

The whole experiment was repeated two times; thus, the optimal repeatability frequency plots were selected. The frequency plots for the same condition were compared with the reference plots to identify the system artefacts.

After the system artefacts were filtered using MATLAB, the frequency with the highest peak in the frequency plot was compared with the input acoustic frequency to determine if the temperature affected frequency characteristics of the DAS system.

The peak amplitude at the corresponding input acoustic frequency in the plot for each experiment condition was recorded in Excel. Bode plots of amplitude vs frequency at different temperatures

were developed to characterise frequency responses of the system. The 3D plot was generated in MATLAB to analyse the correlation between the ambient temperature and the amplitude of acoustic signatures at various acoustic frequency.

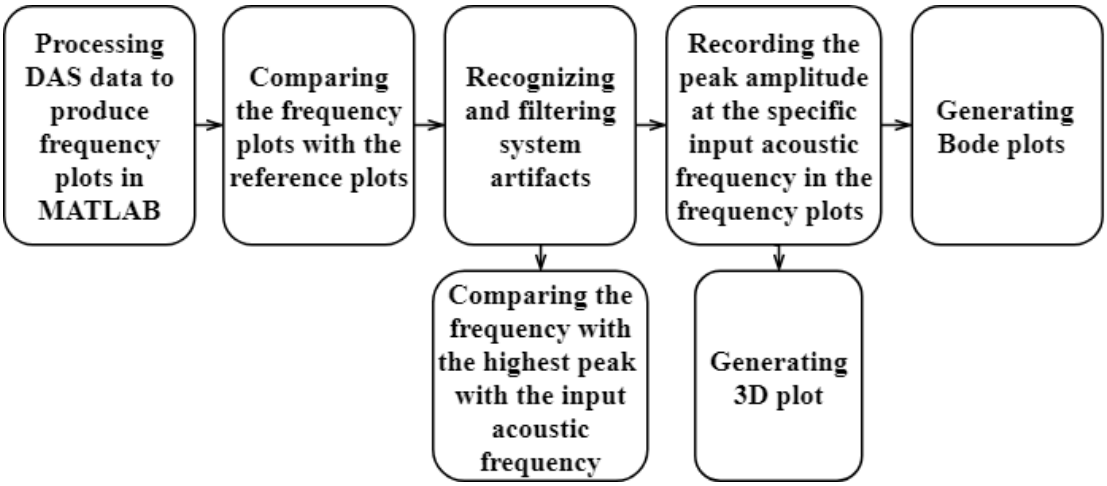

Figure 3.8. A flow chart for data analysis.

CHAPTER 4 RESULTS AND DISCUSSION

4.1 INTRODUCTION

This chapter summarises and analyses the core findings of the laboratory experiment. First, a tap test result is presented to determine the targeted bin location of the fibre in the experiment. Frequency plots are then provided to investigate the temperature effects on frequency characteristics of the DAS system. Finally, the temperature characteristics of the DAS system were examined to identify if the temperature has an impact on the amplitude of acoustic signatures. Potential challenges and constraints of the laboratory experiment are identified based on the results of the experiment.

4.2 TAP TEST RESULT

The tap test result is displayed in a waterfall graph (shown in Figure 4.1) with the x-axis being the fibre distance, y-axis being time and the colour representing the recorded signal intensity, illuminating that the coiled DAS fibre was located within bin 41 to bin 44 that had the highest intensities.

According to fibre installation in Figure 3.6, 1.7 m fibre cable was looped into the DAS fibre coil, and the size of the bin was 0.5 m, meaning that the DAS fibre coil contained 3.4 bins. Therefore, the data acquisition and processing were aimed at bin 42, bin 43 and bin 44 on the fibre.

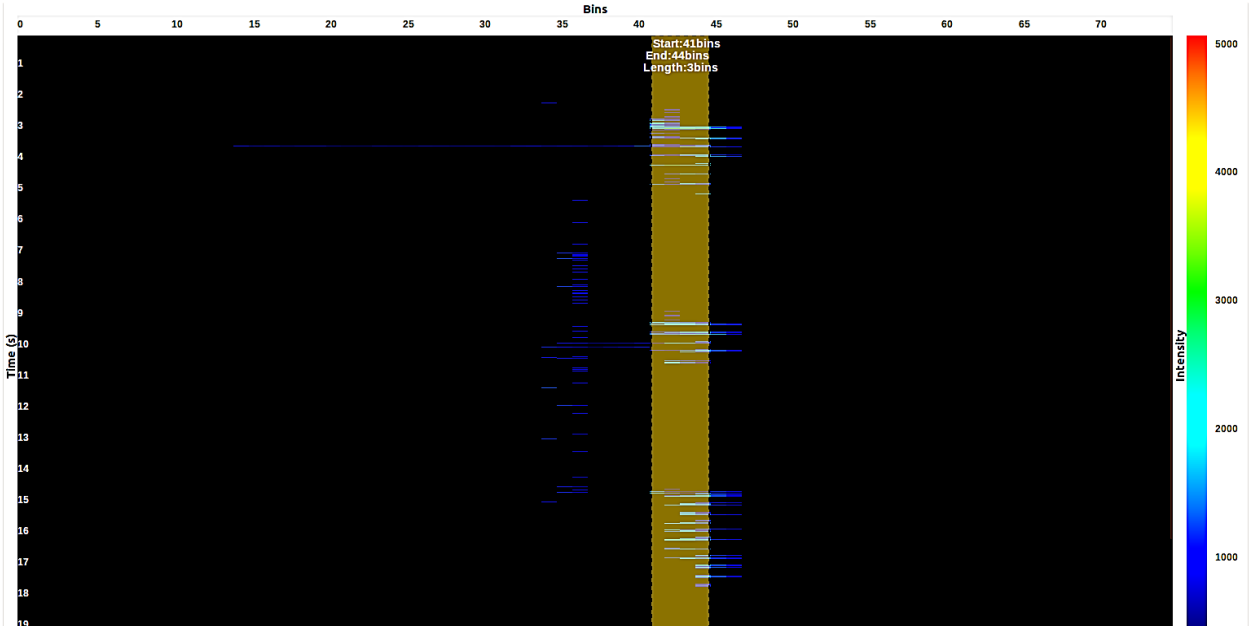

Figure 4.1. A waterfall graph of the tap test result.

4.3 FREQUENCY PLOTS

A total of 336 frequency plots were generated in the project; the details shown below:

$$\text{Total Number of Major Frequency Plots} = \text{Number of bins} \times (\text{Number of Input Frequencies} + \text{Reference}) \times \text{Number of Temperatures} = 3 \times (15 + 1) \times 7 = 336$$

The reference frequency plots were acquired by processing the raw acoustic data that was recorded when the function generator did not generate an acoustic signal to the DAS fibre coil.

Due to a large number of frequency plots being produced, this section only offers the reference frequency plots for bin 43 and the frequency plots for bin 43 when the raw acoustic data were recorded in the condition of an 800 Hz input acoustic frequency transmitted into the DAS fibre coil. The rest of the frequency plots are provided in Appendix.

The reference frequency plot for the temperature of the fibre being 0°C is illustrated in Figure 4.2. It clearly shows that the peaks occur at 0 Hz, 187.1 Hz, 561.1 Hz, 1122 Hz and 1309 Hz even if the reference raw acoustic data was collected without transmitting any input acoustic frequency into the fibre.

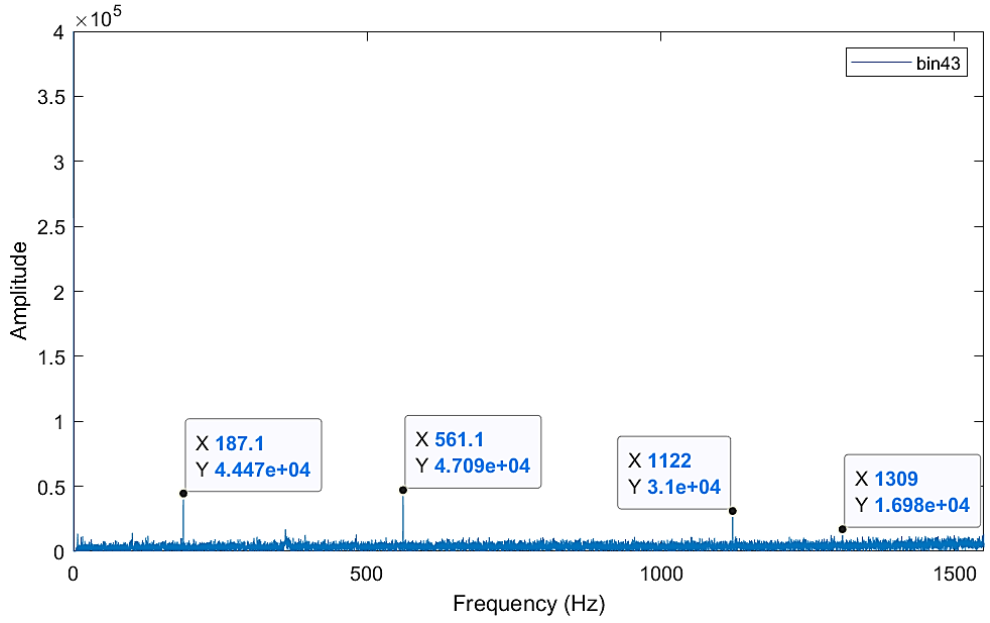

Figure 4.2.Reference frequency plot for bin 43 at 0°C.

The frequency plot with the temperature of the fibre being 0°C is shown in Figure 4.3. The peak at 800 Hz was highlighted in the plot, indicating that the system successfully captured the acoustic signal. By comparing the plot in Figure 4.3 with the one in Figure 4.2, it can be observed that the

peaks exist at 0 Hz, 187.1 Hz, 561.1 Hz, 1122 Hz and 1309 Hz in both frequency plots. It demonstrates that these peaks were generated from the DAS system, which can be identified as system artefacts.

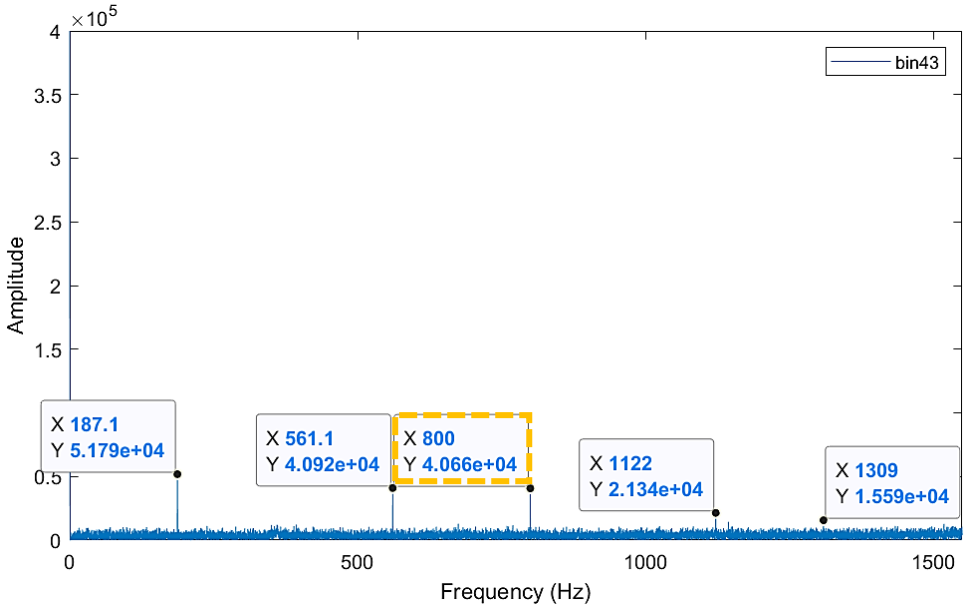

Figure 4.3. Frequency plot for bin 43 at 0°C when the input acoustic frequency was 800 Hz.

To verify the assumption of system artefacts, the reference frequency plot with the fibre temperature of 50°C, and the frequency plot with the input acoustic frequency of 800 Hz and fibre temperature of 50°C are provided in Figure 4.4 and Figure 4.5 respectively. It is visible that the peaks appear at 0 Hz, 187.1 Hz, 561.1 Hz, 1122 Hz and 1309 Hz for both plots, confirming with the ones in Figure 4.2 and Figure 4.3. Thus, the identification of system artefacts is further certified.

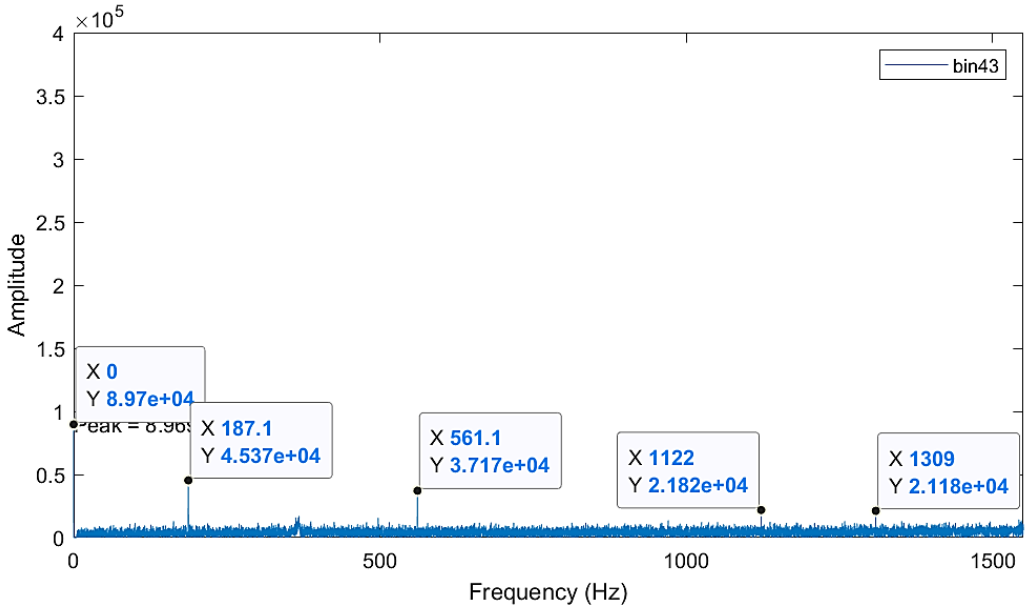

Figure 4.4. Reference frequency plot for bin 43 at 50°C.

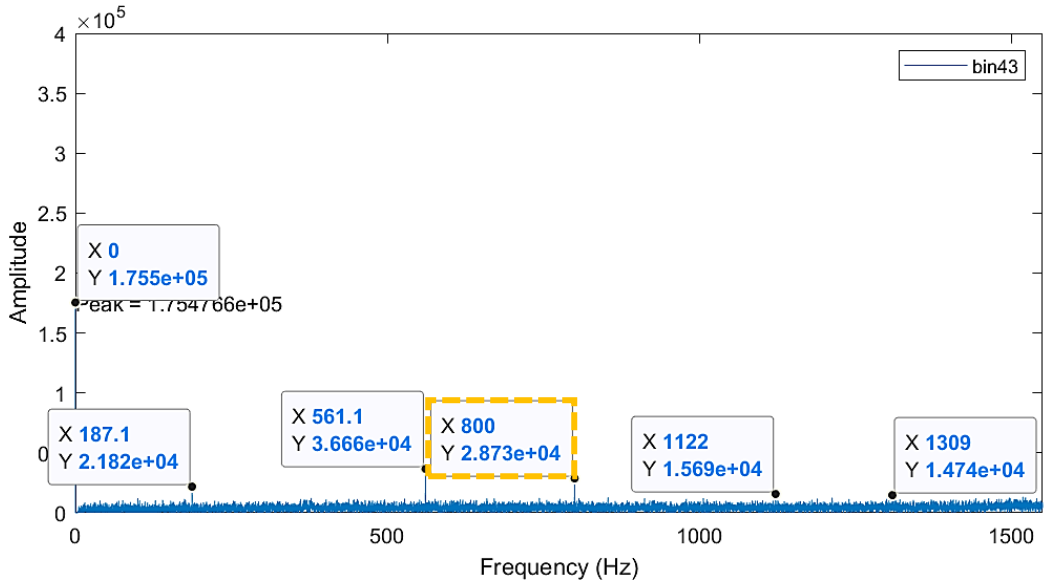

Figure 4.5. Frequency plot for bin 43 at 50°C when the input acoustic frequency was 800 Hz.

In order to analyse the temperature effects on frequency characteristics of the DAS system, the system artefacts were filtered during data processing. The frequency plots for the temperature of the fibre being 10°C, 20°C, 30°C and 40°C are shown in Figure 4.6. Combining with the frequency plots in Figure 4.3, Figure 4.5 and Figure 4.6, it can be observed that a single peak occurs at 800 Hz in each frequency plot, indicating that the system detected the acoustic signal within the fibre with varying temperatures during the experiment. It demonstrates that the ambient temperature does not affect frequency characteristics and signal transmission of the DAS system.

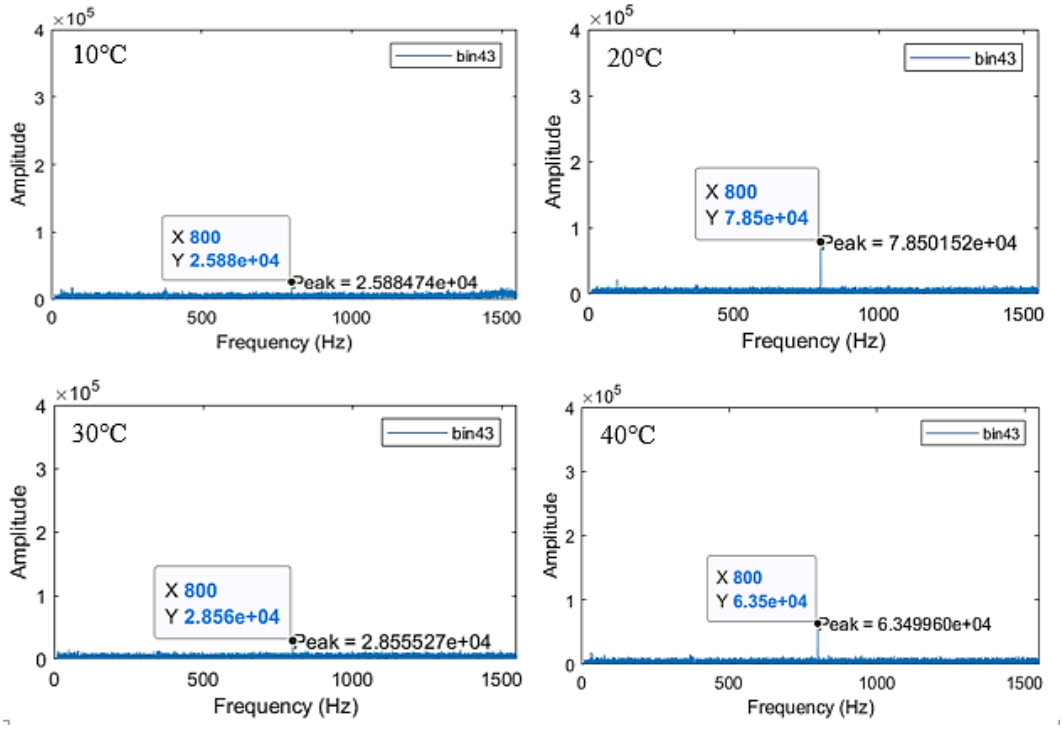

Figure 4.6. Frequency plots for bin 43 at 10°C, 20°C, 30°C and 40°C with the input acoustic frequency of 800 Hz.

4.4 TEMPERATURE CHARACTERISATION

Although the temperature did not have an impact on frequency characteristics of the DAS system, it can be observed from the frequency plots in section 4.3 that the amplitude of the 800 Hz peak is different under various temperatures. To obtain a better understanding of how the system performed at different temperatures, a Bode plot of amplitude against frequency for bin 43 as the temperature of the fibre at 10°C intervals from -10°C to 50°C was developed and shown in Figure 4.7.

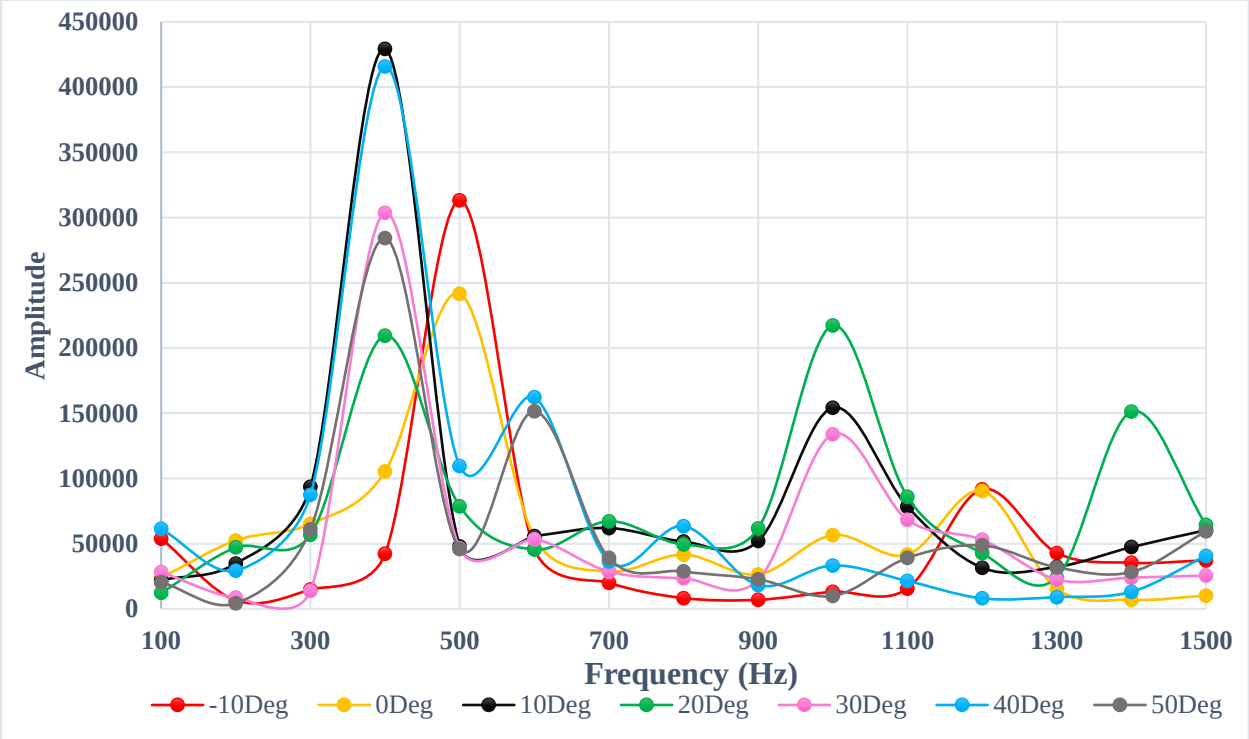

Figure 4.7. A Bode plot of amplitude against frequency as the temperature at 10°C intervals from -10°C to 50°C.

The amplitude for 10°C, 20°C, 30°C, 40°C and 50°C increases dramatically with the input acoustic frequency from 300 Hz up to 400 Hz and declines rapidly as the frequency changing from 400 Hz to 500 Hz. The system appears to respond intensely to the 400 Hz acoustic signal when the temperature of the fibre was above 0°C. It is speculated that the aluminium coil with 9.6 cm in diameter might produce a resonant frequency that intensified the acoustic signal.

However, it can be seen in Figure 4.7 that the amplitude for -10°C and 0°C rises as the acoustic frequency changes from 400 Hz to 500 Hz and the amplitudes decrease when the acoustic frequency changes from 500 Hz to 600 Hz. It seems that the system highly reacted to the 500 Hz acoustic signal as the temperature of the fibre was under 0°C. One of the possibilities is that the frequency response of the speaker was altered with the temperature. The second conjecture is that

the signal attenuated and lost at low temperatures for the single mode jacked optical fibre, as mentioned in Chapter 2 fibre characterisation section. These may explain why the system did not have the same frequency response to the 400 Hz acoustic signal below 0°C and above 0°C.

In Figure 4.7, it shows that the amplitude for the most temperatures fluctuates two times except for that for 20°C that has three fluctuations. The amplitude fluctuates at:

- 400 Hz and 600 Hz, where fibre temperature ≥ 40°C,
- 400 Hz and 1000 Hz, where 0°C < fibre temperature < 40°C, and
- 500 Hz and 1200 Hz, where fibre temperature ≤ 0°C.

A 3D plot was generated and presented in Figure 4.8 to evaluate if the amplitude of the acoustic signature, the ambient temperature and the acoustic frequency have any correlations. It can be seen in Figure 4.8 that three distinct peaks appear at 10°C 400 Hz, 40°C 400 Hz and −10°C 500 Hz.

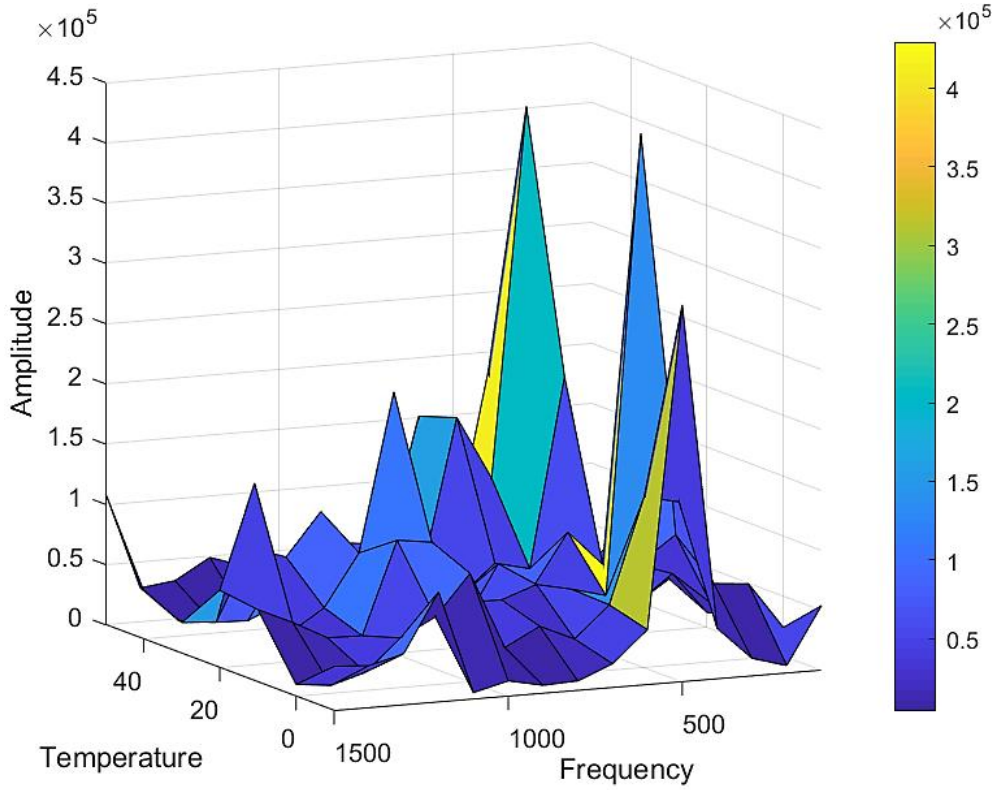

Figure 4.8. A 3D plot generated by using MATLAB for investigating the correlation between amplitude, temperature and frequency.

It is surmised that the variations were caused by the following factors:

- Temperature affected the signal transmission of the speaker.
- Temperature altered the physical property of the aluminium coil.

- Signal attenuation and backscattered light absorption occurred at low temperatures due to the structural properties of the fibre optic cable.
- The DAS fibre was bent onto the aluminium coil, causing the bending loss and signal attenuations.
- The aluminium coil with 9.6 cm in diameter generated the resonant frequency.

By utilising the curve fitting in MATLAB, a polynomial surface was obtained and shown in Figure 4.9. The corresponding equation was generated as follows:

$$\text{Amplitude} = 80500 + 107.9 \times \text{Temperature} - 25.71 \times \text{Frequency}$$

The R-square obtained for that equation was 0.0256, which was far less than one. The higher degree of the polynomial surface was also tested, but the R-square could only reach a maximum of around 0.2. Based on these results, it can be concluded that there was no correlation among the input acoustic frequency, the ambient temperature and the amplitude of acoustic signatures.

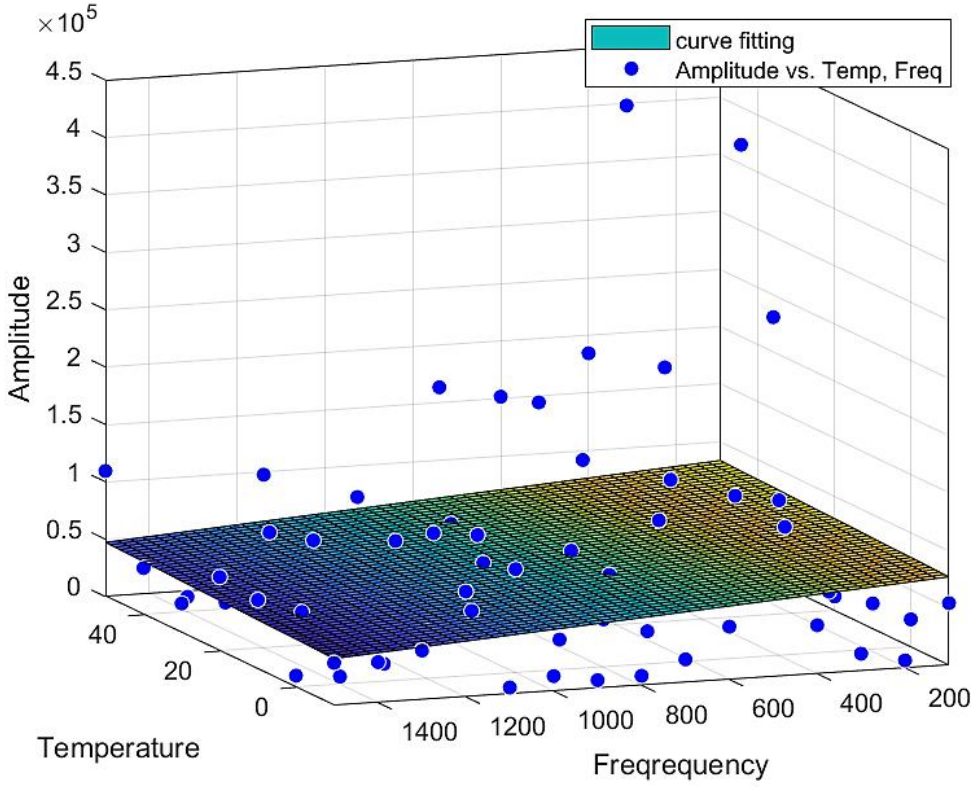

Figure 4.9. Curving fitting for the 3D plot.

CHAPTER 5 CONCLUSIONS AND RECOMMENDATIONS

This project focuses on the study of temperature effects on frequency characteristics of the DAS system and the amplitude of DAS acoustic signatures. A series of laboratory experiments were conducted by transmitting a sine-wave frequency from 100 Hz to 1500 Hz into the coiled fibre at temperatures ranging from -10°C to 50°C. An integrate DAS and DTS system was applied to record the acoustic signals and monitor the temperature of the fibre. By analysing the extracted characteristic frequency plots, the system artefacts were identified. It was also observed that the temperature did not alter the frequency characteristics of the DAS system, but changed the amplitude of the acoustic signatures. A Bode plot was generated to investigate the acoustic transmission characteristics of the DAS system under various temperature. It was found that the amplitude fluctuated at 400 Hz and 600 Hz as the temperature was equal to or greater than 40°C. The amplitude fluctuation occurred at 400 Hz and 1000 Hz, as the temperature being between 0°C and 40°C, and at 500 Hz and 1200 Hz when the temperature was less than or equal to 0°C. The 3D plot and curve fitting plot with its corresponding equation indicated that there was no distinctive correlation between the amplitude of acoustic signatures and the ambient temperature.

In summary, although the temperature has an impact on the properties of an optical fibre, it does not affect the DAS signal transmission. The ambient temperature is one of the factors that cause the amplitude variations in the acoustic signatures. However, many potential factors may influence the results; thus, the relationship between the amplitude of acoustic signatures and the temperature cannot be determined. The potential factors that impacted the outcome of the experiment could be:

- structural properties of the fibre optic cable altered at low temperatures, resulting in the signal attenuation and backscattered light absorption;
- temperature effects on the signal transmission of the speaker;
- the change in physical properties of the aluminium coil at various temperatures;
- the bent fibre causing the bending loss and signal attenuations;
- the resonant frequency generated from the aluminium coil with 9.6 cm in diameter; and
- the temperature fluctuation during the 5 min experimental recording.

The outcome of this project can be served as a starting point for future research. In order to increase the reliability of the DAS system at various temperatures, some recommendations for the future study are provided. It is necessary to conduct a series of experiments using different types of optical fibre and compare their outcomes to determine if different fibre types have distinct effects at various temperatures. The results from the frequency plots identified that the Hawk DAS/DTS system has system artefacts. It is recommended that different types of DAS system can be applied for recording the acoustic data, and the temperature effects on their performance can be compared and characterised. It was surmised that the aluminium coil with 9.6 cm in diameter applied in the experiment generated the resonant frequency, thus intensifying the signal transmission. To verify this hypothesis, it is recommended to utilise the metal coil with different diameters in the experiment and compare the results. It was noticed that the temperature of the chamber could decrease by 1°C to 2°C during the 5 min recording time in the experiment, which could result in transmission loss and changes in the refractive index of the fibre. Therefore, it is essential to make sure that the temperature stays constant during the data recording in the future experiment. The theoretical expression shows that temperature variations cause changes in the refractive index of an optical fibre, thus changing the time-of-flight. The changes of time-of-flight also depend on the distance a laser pulse propagating through the fibre. Therefore, it is worthwhile placing a longer length of the optical fibre (a minimum of 1.2 km) in the climatic chamber to investigate the distinction it produces. Because of the time constraints, the performance of the DAS system was not tested at a broader range of temperatures. For future research, it is suggested to increase the range of the temperature variation and reduce the temperature interval.

REFERENCES

AKKERMAN, J. & PRAHL, F. 2013. Fibre Optic Sensing for Detecting Rock Falls on Rail Rights of Way. 1099 - 1118.

CANNON, R. T. & AMINZADEH, F. 2013. Distributed Acoustic Sensing: State of the Art. *SPE Digital Energy Conference.* The Woodlands, Texas, USA: Society of Petroleum Engineers.

DALEY, T. M., FREIFELD, B. M., AJO-FRANKLIN, J., DOU, S., PEVZNER, R., SHULAKOVA, V., KASHIKAR, S., MILLER, D. E., GOETZ, J., HENNINGES, J. & LUETH, S. 2013. Field testing of fibre-optic distributed acoustic sensing (DAS) for subsurface seismic monitoring. *The Leading Edge,* 32**,** 699-706.

DUCKWORTH, G. L. & KU, E. M. 2013. *OptaSense distributed acoustic and seismic sensing using COTS fibre optic cables for infrastructure protection and counter terrorism*, SPIE.

GIUNTA, G., DIONIGI, F., BASSAN, A., VENEZIANI, M., BERNASCONI, G., DEL GIUDICE, S., ROVETTA, D., SCHIAVON, R. & ZANON, F. Third Party Interference And Leak Detection On Buried Pipelines For Reliable Transportation Of Fluids. Offshore Mediterranean Conference and Exhibition, 2011 Ravenna, Italy. Offshore Mediterranean Conference, 12.

GOLNABI, H. & SHARIFIAN, M. 2013. Investigation of bending and temperature effects in optical fibres. *Microwave and Optical Technology Letters,* 55**,** 82-86.

HARTOG, A. H. 2018. *An Introduction to Distributed Optical Fibre Sensors*, CRC Press.

HAWK 2017. Fibre Optic Sensing. *In:* SENSING, P.-F. O. (ed.). Hawk Measurement Systems.

HE, Z., LIU, Q., FAN, X., CHEN, D., WANG, S. & YANG, G. Fibre-optic distributed acoustic sensors (DAS) and applications in railway perimeter security. SPIE/COS Photonics Asia, 2018 Beijing, China SPIE.

HICKE, K., HUSSELS, M.-T., EISERMANN, R., CHRUSCICKI, S. & KREBBER, K. 2017. Distributed Fibre Optic Acoustic and Vibration Sensors for Industrial Monitoring Applications.

HILL, D. Distributed Acoustic Sensing (DAS): Theory and Applications. Frontiers in Optics 2015, 2015/10/18 2015 San Jose, California. Optical Society of America, FTh4E.1.

HUSSAINI, U. 2017. *General structure of optical fibres* [Online]. Available: https://www.technobyte.org/2016/11/general-structure-of-optical-fibers [Accessed June 10 2019].

HUSSELS, M.-T., CHRUSCICKI, S., HABIB, A. & KREBBER, K. Distributed acoustic fibre optic sensors for condition monitoring of pipelines. Sixth European Workshop on Optical Fibre Sensors (EWOFS'2016), 2016 Limerick, Ireland. SPIE, 5.

ISMAIL, M. 2009. *Thermal Effects in Optical Fibres.* Master of Science in Electronics and Communications Engineering, Arab Academy for Science and Technology & Maritime Transport.

JAASKELAINEN, M. 2009. *Fibre optic distributed sensing applications in defence, security, and energy,* SPIE.

JASNY, J., NICKEL, B. & BOROWICZ, P. 2004. Wavelength- and temperature-dependent measurement of refractive indices. *Journal of the Optical Society of America B,* 21**,** 729-738.

KATSUYAMA, Y., MITSUNAGA, Y., ISHIDA, Y. & ISHIHARA, K. 1980. Transmission Loss of Coated Single-Mode Fiber at Low Temperatures. *Applied Optics,* 19**,** 4200-4205.

KIMBELL, F. J. 2013. *History and analysis of distributed acoustic sensing (DAS) for oilfield applications.* Master of Science, Texas A&M University.

KOELMAN, J. V. V., LOPEZ, J. L. & POTTERS, H. 2011. Fibre Optic Technology for Reservoir Surveillance. *International Petroleum Technology Conference.* Bangkok, Thailand: International Petroleum Technology Conference.

LI, M., WANG, H. & TAO, G. 2015. Current and Future Applications of Distributed Acoustic Sensing as a New Reservoir Geophysics Tool. *The Open Petroleum Engineering Journal* 8**,** 272-281.

LIU, A. 2014. *Three Common Types of Fibre Optic Cable* [Online]. Available: http://www.cables-solutions.com/three-common-types-of-fiber-optic-cables.html [Accessed 2019].

MATEEVA, A., LOPEZ, J., POTTERS, H., MESTAYER, J., COX, B., KIYASHCHENKO, D., WILLS, P., GRANDI, S., HORNMAN, K., KUVSHINOV, B., BERLANG, W., YANG, Z. & DETOMO, R. 2014. Distributed acoustic sensing for reservoir monitoring with vertical seismic profiling. *Geophysical Prospecting,* 62**,** 679-692.

MESTAYER, J., COX, B., WILLS, P., KIYASHCHENKO, D., LOPEZ, J., COSTELLO, M., BOURNE, S., UGUETO, G., LUPTON, R., SOLANO, G., HILL, D. & LEWIS, A. 2011. Field trials of distributed acoustic sensing for geophysical monitoring. *SEG Technical Program Expanded Abstracts 2011.* Society of Exploration Geophysicists.

MINING3 2016. Mining3 Risk Assessment Matrix. *In:* TEMPLATE, W. F. R. A. (ed.).

MOLENAAR, M. M., FIDAN, E. & HILL, D. 2012. Real-Time Downhole Monitoring Of Hydraulic Fracturing Treatments Using Fibre Optic Distributed Temperature And Acoustic Sensing. *SPE/EAGE European Unconventional Resources Conference and Exhibition* Vienna, Austria: Society of Petroleum Engineers.

MORAN, K. *Digital Acoustic Sensing: Leading an Ear.* Viterbi School of Engineering

PIMENTEL, M. DAS (Distributed Acoustic Sensing) - Pipeline Monitoring and the Blue Colour of the Sky. Pipeline Technology Conference 2017, 2 May 2017. 11.

SILKINA, T. 2014. *Application of distributed acoustic sensing to flow regime classification.* Department of Petroleum Technology and Applied Geophysics (NTNU).

SYSTEMS, H. M. 2018. *User Manual Praetorian Distributed Acoustic and Temperature Fibre Optic Sensing,* Hawk Measurement System Pty. Ltd.

TATEDA, M., TANAKA, S. & SUGAWARA, Y. 1980. Thermal characteristics of phase shift in jacketed optical fibers. *Applied Optics,* 19**,** 770-773.

TEJEDOR, J., MARTINS, H. F., PIOTE, D., MACIAS-GUARASA, J., PASTOR-GRAELLS, J., MARTIN-LOPEZ, S., GUILLÉN, P. C., DE SMET, F., POSTVOLL, W. & GONZÁLEZ-HERRÁEZ, M. 2016. Toward Prevention of Pipeline Integrity Threats Using a Smart Fiber-Optic Surveillance System. *Journal of Lightwave Technology,* 34**,** 4445-4453.

WANG, Z. Y., QIU, Q. & SHI, S. J. 2014. Temperature dependence of the refractive index of optical fibres. *Chinese Physics B,* 23**,** 034201.

WILSON, P., BROOKS, T., HOEHN, K., GIANG, L. & VIEIRA, F. 2018. Distributed Acoustic Conveyor Monitoring Phase 2 Final Report. *ACARP Project C25054.* Mining3.

WILSON, P., PROCHON, E., VIEIRA, F., BROOKS, T., GIANG, L., AMANZADEH, M., ADAM, S. & AMINOSSADATI, S. 2016. Distributed Acoustic Conveyor Monitoring Phase 1 Final Report. *ACARP PROJECT C24014.* CRCMining and The University of Queensland.

YEUNG, W. F. & JOHNSTON, A. R. 1978. Effect of temperature on optical fibre transmission. *Applied optics,* 17**,** 3703-3705.

APPENDIX A PROJECT MANAGEMENT

A.1 PROJECT TIMELINE

The project is separated into four major stages:

- research and experiment preparation,
- experimentation,
- data processing and analysing, and
- final report generation and presentation.

In order to accomplish the project within the allocated time, it is critical to managing the project efficiently with schedules. A project timeframe is presented in Figure A.1, including tasks, milestones, dependencies, their corresponding dates, percent complete and durations.

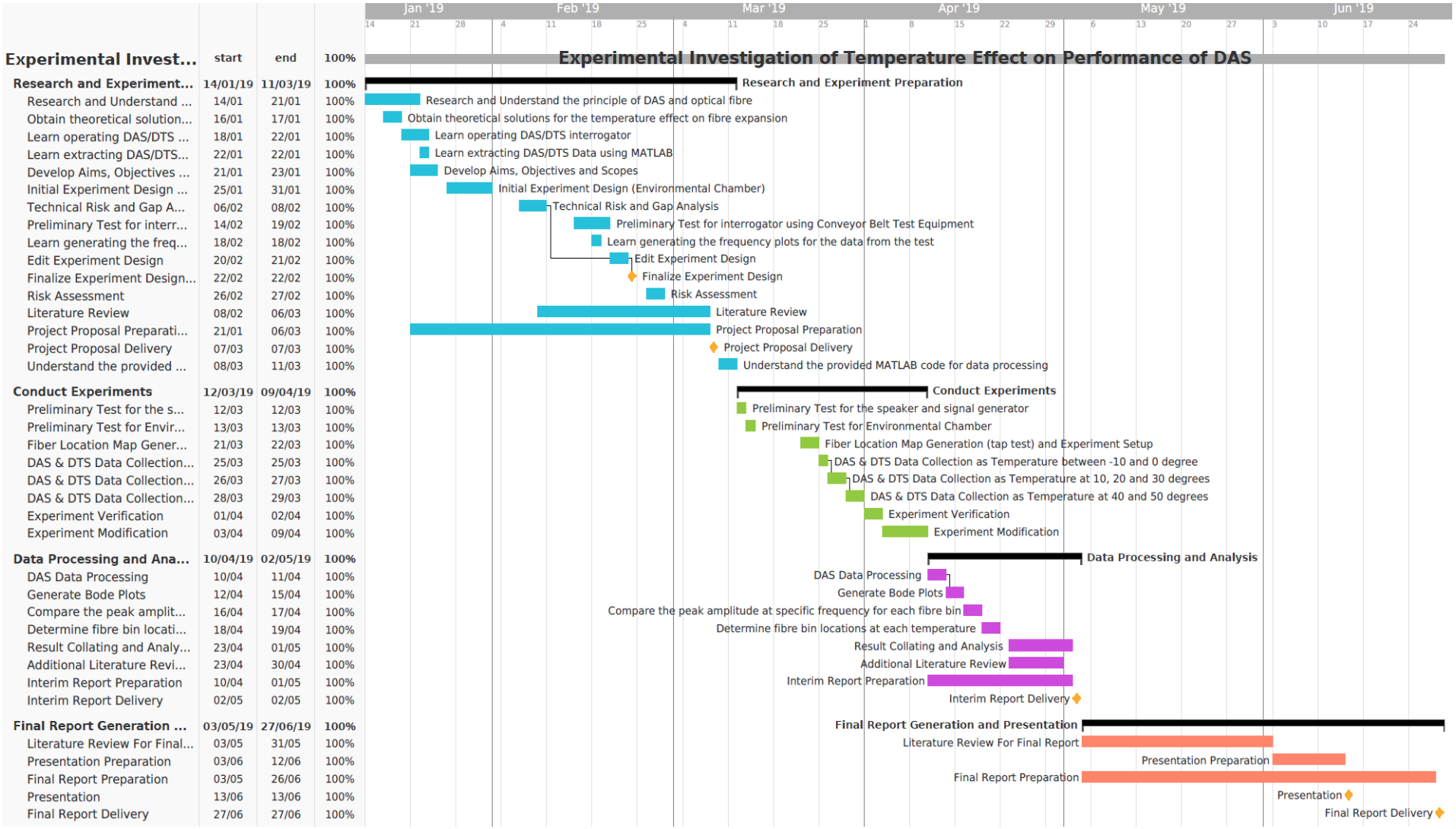

Figure A.1 Gantt Chart for project timeline

A.2 RISK MANAGEMENT

The project risks are categorised as technical uncertainties (shown in Table A.1) that may affect the achievement of the project goals and potential hazards related to safety, cost and planning (shown in Table A.2). Table A.3 measures the potential severity with levels of likelihood and consequence of these risks and thus defines the overall risk level.

A.2.1 Technical Risks

To promote the success rate of the project, it is essential to recognise and mitigate the uncertainties and concerns that would arise during the experimental investigation. The uncertainties, risk rankings and the corresponding risk mitigation strategies are addressed in Table A.1.

Table A.1. Technical risk ranking and the corresponding mitigation strategies

Uncertainty /Concern	**Initial Proposed Control**	**Likelihood**	**Consequence**	**Risk Ranking**	**Mitigation Strategy**	**Residual Likelihood**	**Residual Consequence**	**Residual Risk Ranking**
The actual temperature that the optical fibre receives from the environment chamber.	Compare the DTS profile with the temperature setting of the environmental chamber	C	1	22 Low	Thermistors can also be utilised for double checking the temperature of the optical fibre inside the chamber	E	1	25 Low
The frequency and intensity of the signal in speaker transmission are attenuated.	The same speaker is applied throughout the experiment to keep experiment consistency	C	2	18 Medium	Read the frequency response curve of the speaker on the datasheet before commencing the experiment	C	1	22 Low
The consistency of the frequency and intensity of the signal that the optical fibre in the environmental chamber receives	Test with a tightly aluminium-coiled fibre coil and a speaker placed on the top of the coil	C	2	18 Medium	Additional test with a loosely coiled fibre and the speaker placed in the middle of the fibre	D	2	21 Low
The connection of the speaker is not stable.	Check the connection each time before recording the data	A	2	10 High	Solder the speaker wire to make the connection more stabilized.	E	2	23 Low

A.2.2 Safety, Cost and Scheduling Risks

Table A.2 identifies, evaluates and controls the potential risks associated with safety, cost and project schedule.

Table A.2. Safety, cost and schedule risk ranking and the corresponding mitigation strategies

Task Activity	Potential Hazard	Initial Proposed Control	Risk Area	Likelihood	Consequence	Risk Ranking	Mitigation Strategy	Residual Likelihood	Residual Consequence	Residual Risk Ranking
Working with fibre optic DAS/DTS interrogator	When the interrogator is on, the fibre optic laser behind the interrogator has sufficient optical power to damage human eyes.	Read the fibre optic safety rule. Avoid looking straight into the laser light.	PAS	C	3	13 High	Wear safety glasses and avoid working with the bare fibre.	D	2	21 Low
	Fibre is damaged. The fibre must, therefore, be reordered and replaced. In addition, the tap test must be redone.	Read the installation manual.	AS	C	2	18 Medium	Ask the experienced person to assist in connecting the fibre.	D	1	22 Low
Connecting electric cables	An electrical fault occurs due to earth leakage, causing injury.	UQ conducts ELCB testing every six months.	PAS	E	4	16 Medium	Double check the cable prior to power connection.	E	4	16 Medium
Operating environmental chamber	Open the chamber at high temperature without disconnecting power, causing scalding.	Pause/stop the chamber before opening its door.	PAS	C	2	18 Medium	Remove the fibre until the chamber temperature is cooled down.	D	2	21 Low
	Environmental chamber power failure, terminating the experiment.	Report the issue to the supervisor immediately.	S	C	3	13 High	Avoid setting the temperature above 50°C.	D	3	17 Medium
Processing data	Laptop memory is full due to the massive data files. The laptop freezes up, causing project delay	Clean up the memory space before processing data.	S	C	3	13 High	Process the data in parts to achieve the fastest performance	D	2	21 Low

Table A.3. Risk matrix (Mining3, 2016)

		Consequence				
		1 Insignificant	**2 Minor**	**3 Moderate**	**4 Major**	**5 Catastrophic**
Definition	**(P) People**	Slight injury or health effects – first aid	Minor injury or health effects – minor medical treatment	Significant injury or health effects – restricted work	Permanent disability	Fatality or multiple fatalities
	(A) Asset Damage	Slight damage less than $5000	Minor damage $5000 to $50,000	Local damage $50,000 to $500,000	Major damage $500,000 to $1M	Extreme damage more than $1M
	(S) Schedule	Insignificant project delay	Minor delays but able to meet critical milestones	Project delays, but the timeline is recoverable with further effort	Major delays. The project timeline is critically affected	The project is not completed and cannot meet key milestones
	(T) Technical	Slight impact on achieving project objectives but can still be met in full	Minor impact on achieving project objectives but core objectives can still be met	Core objectives will not be met. There is an alternative solution but are undesirable	Severe impact on achieving project objectives. There is no alternative solution	Significant impact on achieving project objectives. The objectives are not realisable
Likelihood	**A Almost certain**	15 (M)	10 (H)	6 (H)	**2 (Ex)**	**1 (Ex)**
	B Likely	19 (M)	14 (M)	9 (H)	**4 (Ex)**	**3 (Ex)**
	C Possible	22 (L)	18 (M)	13 (H)	8 (H)	**5 (Ex)**
	D Unlikely	24 (L)	21 (L)	17 (M)	12 (H)	7 (H)
	E Rare	25 (L)	23 (L)	20 (M)	16 (M)	11 (H)

Risk Ranking	**Risk Level**
Extreme (1-5)	Immediate correction required -Eliminate, avoid or implement specific plans/ Standards to manage & monitor
High (6-13)	Should receive attention as soon as possible - Proactively manage
Medium (14-20)	Should be dealt with as soon as possible but the situation is not an emergency - proactively manage
Low (21-25)	The risk usually is acceptable - Monitor & manage as appropriate

A.3 OPPORTUNITIES

In addition to analysing negative project risks, it is also crucial to identify opportunities that may provide the project with a positive impact. The potential opportunities are described below:

- the outcome of the investigation further enhances the precision of DAS performance, which offers broad prospects for many applications;
- the project outcome has an opportunity to provide a platform for product implementation; and
- the final report can be published in a research journal on this project topic in order to extend the current literature.

APPENDIX B PROFESSIONAL DEVELOPMENT

B.1 KEY LEARNING EVENT IN FEBRUARY – GIVEN TASK ASSIGNMENT

Table B.1. EA Stage 1 competencies developing for key learning event in February

EA Stage 1 competencies developing	Description
EA 1.2	Conceptual understanding of the mathematics, numerical analysis, statistics and computer and information sciences which underpin the engineering discipline.
EA 1.4	Discernment of knowledge development and research directions within the engineering discipline.
EA 3.5	Orderly management of self, and professional conduct.
EA 3.6	Effective team membership and team leadership.

Situation:

In the first week of the placement, I was given a task assignment to theoretically estimate the length that a 10 km optical fibre would expand when the temperature increases 40 degrees. I was not provided with any references or formula. I had limited background knowledge about optical fibre at that time, so I read many papers to get a better understanding of the principles of it before commencing the task. However, I was still struggling to find the related formulas.

Effect:

I felt frustrated that I spent almost one day on searching and reading the related journal articles but still could not find any useful ones. I realised that I should stop to think of the reason causing this problem, whether it was due to the difficulty of the task or the wrong keywords that I put in the search engine.

Action:

To solve this problem, I asked one of the co-workers what keywords he would put in the search engine if he had the same task as mine. By taking his suggestions, I found some pieces of the literature demonstrated that the temperature would affect the reflective index of the optical fibre and some other journal articles proved that the change of the reflective index would have an impact on the length of the optical fibre. By knowing these concepts, I quickly searched out the derivations of formulas. I collected three related papers, utilised the summarised equations to develop a MATLAB code and generated plots. The other co-workers confirmed the results I got.

Learning:

From this task assignment, not only my computational skills and modelling skills that I have already gained at the university were developed, but also my research skills were significantly improved. I learnt that it is essential to have good literature searching ability for students, researchers or any experts. Search competency is like learning a language, and it has to be established through exercise and with the guidance of mentors. Mastering this skill will strengthen my capability for critical thinking and highly increase my work efficiency in the future.

B.2 KEY LEARNING EVENT IN MARCH – CONDUCTING AN EXPERIMENT

Table B.2. EA Stage 1 competencies developing for key learning event in March

EA Stage 1 competencies developing	Description
EA 1.2	Conceptual understanding of the mathematics, numerical analysis, statistics and computer and information sciences which underpin the engineering discipline.
EA 1.3	In-depth understanding of specialist bodies of knowledge within the engineering discipline.
EA 1.6	Understanding of the scope, principles, norms, accountabilities and bounds of sustainable engineering practice in the specific discipline.
EA 2.1	Application of established engineering methods to complex engineering problem solving.
EA 2.2	Fluent application of engineering techniques, tools and resources.
EA 3.1	Ethical conduct and professional accountability.

Situation:

I was assigned a task of planning and conducting an experiment using Distributed Acoustic Sensing (DAS) interrogator and conveyor test equipment to compare three types of the clip that attach optical fibre on the conveyor frame. When I was about to do the experiment, a DAS team member stopped me and guided me to complete Take Five risk assessment.

Effect:

This experience cautioned me the importance of safety and necessity of having risk management prior to the experiment. I felt ashamed that I forgot to apply what I learnt from the student induction to practice.

Action:

I took the Take Five booklet with me whenever I used the lab and filled it out seriously.

Learning:

From this experience, I appreciated the significance of applying the risk management concept to practice and the principle of health and safety responsibilities. I will take this lesson and keep safety in mind whenever I need to conduct an experiment. I believe that this lesson will be integrated into my future engineering career.

B.3 KEY LEARNING EVENT IN APRIL – CONDUCTING PROJECT EXPERIMENT

Table B.3. EA Stage 1 competencies developing for key learning event in April

EA Stage 1 competencies developing	Description
EA 2.2	Fluent application of engineering techniques, tools and resources.
EA 2.3	Application of systematic engineering synthesis and design processes.
EA 3.5	Orderly management of self and professional conduct.

Situation:

At the end of March, I conducted my placement project in the fibre-optic sensing laboratory at QCAT. During the experiment setup, I only tested a speaker once before I placed it inside an environmental chamber. I spent a week to record the acoustic data from the Distributed Optical Fibre Acoustic Sensing system. However, when I processed the data, I could not find a peak at a specific frequency (the input frequency of the speaker in the frequency plot). In order to detect the problem, I modified the experiment method and recording time. I spent another two days to record enough data and then implemented the data processing, but the issue was not resolved.

I started to check the fibre and speaker connection; then I found that the problem was caused by the unstable speaker connection.

Effect:

I was very disappointed in myself that the time I spent on collecting the raw acoustic data was far longer than I expected. If I could check the setup and the connection every time before recording the data, the experiment would be finished by now.

Action:

I reconnected the speaker, ensuring that the connection is stable and tested it every time before I started a new recording. I also adjusted my project timeline to make sure that I have enough time to complete the experiment and analyse results.

Learning:

From this event, I appreciated the preciousness of time and the importance to be circumspection during the experiment. I realised that it is significantly essential to check the experiment setup and cable connections every time prior to recording the data. To redeem the amount of time that I wasted in the experiment, I will manage the time efficiently from now on and learn from this lesson to avoid making the same mistake in the future.

B.4 Key Learning Event in May – Discussing the Experiment Results with Supervisor

Table B.4. EA Stage 1 competencies developing for key learning event in May

EA Stage 1 competencies developing	Description
EA 1.4	Discernment of knowledge development and research directions within the engineering discipline.
EA 2.1	Application of established engineering methods to complex engineering problem solving.
EA 2.2	Fluent application of engineering techniques, tools and resources.
EA 3.6	Effective team membership and team leadership.

Situation:

In the mid-April, all the resulting data were collected and plotted using Excel. I generated 15 plots for examining temperature effects on bin locations of the optical fibre, but I did not find any correlations.

Effect:

I was a bit disappointed with this experiment result. Theoretically, the fibre length would be expanded as the temperature increased, thus shifting the bin locations within the optical fibre.

Action:

I talked to my placement supervisor about the experiment results to seek advice. From the discussion, I realised that not all the experiment results comply with the theory due to experimental limitations. If I utilised 1 km of fibre in the climatic chamber, which was not realistic in the laboratory experiment, I would see a precise result. The supervisor suggested that I could write this issue in the discussion section of the report and make some recommendations for future experiments.

Learning:

From this event, I gained the experience of how to deal with the unexpected experiment results in the future. This experience also built up my confidence in writing the project final report.

B.5 Key Learning Event in June – Having a Presentation in the Technical Group Meeting

Table B.5. EA Stage 1 competencies developing for key learning event in June

EA Stage 1 competencies developing	Description
EA 3.2	Effective oral and written communication in professional and lay domains.
EA 3.5	Orderly management of self and professional conduct.
EA 3.6	Effective team membership and team leadership.

Situation:

At the end of May, my placement supervisor provided me with an opportunity to present placement project outcomes in a technical group meeting. I prepared PowerPoint slides that included the experimental methodology, results, discussion, conclusion and recommendations. I also rehearsed my presentation several times before the technical meeting.

Effect:

When it came to the presentation, I was a bit nervous at the beginning, and my English pronunciation became unclear. I tried to stay calm and adjust this speech impediment. As the presentation progressed, I felt much more confident.

Action:

After the presentation, I asked my supervisor and the other members for the feedback. They provided me with suggestions on how I could present the results more convincingly.

Learning:

From this experience, I appreciate the opportunity and valuable advice that my supervisor and the other technical team members provided. I gained experience in presenting experimental outcomes succinctly and clearly in front of experts. My communication skills have improved, and I feel more confident to prepare for my upcoming oral presentation at university.

APPENDIX C MATLAB CODE FOR THEORETICAL COMPUTATION

```
clear;
close all;

format long
% Material of Optical Fiber is SiO2
ionicBond_fraction = 0.514;
q = ionicBond_fraction * 2 * 1.602e-19; % total electric quantity
permittivity = 8.854189e-12; % vacuum permittivity (F/m)
a = 1.779e2;  % (J/m^2)
b = 1.265e12; % (J/m^3)
Ec = 1e11;    % local electric field (V/m)
r0 = 1.6e-10; % length of each Si-O bond (m)
N = 0.2/r0^3; % average number density (m-3)of the Si-O bonds along
              % the direction of a local electric field Ec
kB = 1.38064852e-23;  % Boltzmann's constant (J/K)

A = q^2/a;
B = (3*q*b*kB)/(Ec*(a^2));

% section1 = 3*N*A/(3*permittivity - N*A);
% section2 = 3*N*B/(3*permittivity - N*A);
section1 = sqrt((3*permittivity + 2*N*A)/(3*permittivity - N*A));
section2 = (3*N*B)/(2*sqrt((3*permittivity + 2*N*A)*(3*permittivity - N*A)));

c = 3e8;   % speed of light in vacuum (m/s)
% L = 1200;     % length of fiber (m)
Tmax = 50; % (degree)
v_system = c*2/3;

T_C = 0;   % temperature at 0 degree
% n0 = sqrt(1 + section1 + section2*(T_C + 273.15)); % refractive index at 0 degree
% n0 = section1 + section2*(T_C + 273.15); % refractive index at 0 degree
n0 = 1.47269 + (7.09780e-6)*(T_C + 273.15); % refractive index at 0 degree
v0 = c/n0; % speed of light at 0 degree

T_init = -10;   % temperature at 0 degree
% n_init = sqrt(1 + section1 + section2*(T_init + 273.15)); % refractive index at -10 degree
% n_init = section1 + section2*(T_init + 273.15); % refractive index at -10 degree
n_init = 1.47269 + (7.09780e-6)*(T_init + 273.15); % refractive index at -10 degree
v_init = c/n_init; % speed of light at 0 degree
```

```
L = zeros(1, 120);
T_K = zeros(Tmax, length(L));
n = zeros(Tmax, 1);
v = zeros(Tmax, 1);          % speed of light in fiber (m/s)
delay = zeros(Tmax,length(L));      % fiber delay (s)
expansion = zeros(Tmax, length(L)); % expansion of the fiber (m)
delay0 = zeros(1, length(L));
expansion0 = zeros(1, length(L));

for m = 2:length(L)
    L(1) = 10;
    L(m) = L(m-1) + 10;
end

for m = 1:length(L)
    for T = 1:Tmax
        T_K(T) = T + 273.15;
    %     n(T) = sqrt(1 + section1 + section2*T_K(T));
    %     n(T) = section1 + section2*T_K(T);
        n(T) = 1.47269 + (7.09780e-6)*T_K(T);
        v(T) = c/n(T);
        delay(T, m) = L(m)*(n(T) - n_init)/v(T);
    %     expansion(T) = L * (n(T) - n_init);
        expansion(T, m) = delay(T, m) * v_system;
    end
    delay0(m) = L(m)*(n0 - n_init)/v0;
    expansion0(m) = delay0(m) * v_system;
end
```

```
figure, subplot(1,2,1), plot([-10 0], [n_init n0],'b'), hold on, plot(n);
title('Refractive Index at Different Temperature');
xlabel('Temperature (degree)');
ylabel('Refractive Index');
xlim([-10 50]);
hold off;

subplot(1,2,2), plot([-10 0], [v_init v0], 'b'), hold on, plot(v);
title('Speed of Light in Fiber at Different Temperature');
xlabel('Temperature (degree)');
ylabel('Speed of light in Fiber (m/s)');
xlim([-10 50]);
hold off;

figure, subplot(1,2,1), plot([-10 0], [0 delay0], 'b'), hold on, plot(delay);
title('Fiber Delay at Different Temperature');
xlabel('Temperature (degree)');
ylabel('Fiber Delay (s)');
xlim([-10 50]);
hold off;

subplot(1,2,2), plot([-10 0], [0 expansion0], 'b'), hold on, plot(expansion);
title('Expansion of Fiber at Different Temperature');
xlabel('Temperature (degree)');
ylabel('Fiber Expansion (m)');
xlim([-10 50]);
hold off;
```

APPENDIX D PLOTS OF AMPLITUDE VERSUS TEMPERATURE AT DIFFERENT FREQUENCIES